Palaeobotanist 48 (1999) : 183-209
0031-0174/99/183-209 $2.00

Subduction and collision related magmatism in the Shyok Suture and eastern Karakoram

RAKESH CHANDRA[1], RAJEEV UPADHYAY[2] AND ANSHU K. SINHA[3]

[1] *Government Degree College, Dharamsala 176215, India.*
[2] *Institute of Geology, ETH-Zentrum, 8092 Zurich, Switzerland.*
[3] *Birbal Sahni Institute of Palaeobotany, Lucknow 226007, India.*

(Received 4 August 1999; revised version accepted 6 October 1999)

ABSTRACT

Chandra R, Upadhayay R & Sinha AK 1999. Subduction and collision related magmatism in the Shyok Suture and eastern Karakoram. Palaeobotanist 48(3) : 183-209.

The Shyok Suture is represented by distinct sets of volcano-plutonic rock assemblages. The high-Mg tholeiitic basalt and calc-alkaline andesites of the Shyok Volcanics have a subduction zone chemical signatures. The REE data on tholeiitic basalt suggest chemical affinity between primitive N-MORB to E-MORB. The calc-alkaline andesites, however, resembles to transitional nature of basalt between E-MORB to OIB. The geochemical data and regional tectonic setting suggest a close similarity between the Shyok Volcanics of northern Ladakh and Chalt Volcanics of Kohistan.

The mildly deformed trondhjemite-tonalite-granodiorite of the Tirit Granitoids are composite plutons located south of the Shyok Suture melange. These granitoids are subalkaline, I-type and represented by volcanic arc chemical signatures. The regional tectonic setting, the nature of occurrence and the composition of Tirit Granitoids are similar to the plutonic suites of northern Kohistan (Gindai, Matum Das and Nomal plutons).

The eastern Karakoram Batholith is dominated by quartz monzonite-tonalite-granodiorite and granite. The subalkaline to calc-alkaline Karakoram Batholith is constituted by both I-and S-type granitoids with volcanic arc and syn-collision chemical signatures. REE data suggest that the I-type granitoids of eastern Karakoram are calc-alkaline magmatism of a subduction zone environment. In contrast, most of the S-type granitoids are crust-derived peraluminous granitoids. New Rb/Sr isotopic whole rock age data indicates that a S-type intrusive phase was active in the eastern Karakoram region during 83±9 Ma. The syn-collision nature of these granitoids are similar to those of north Sost pluton and Karambar pluton of northern Kohistan. This indicates that the collision between Kohistan-Ladakh arc and Karakoram block was active during 83±9 Ma.

Key-words—Subduction, Collision, Magmatism, Shyok Suture, Karakoram, India.

सारांश

श्योक सन्धिस्थल एवं पूर्वी काराकोरम में अपक्षय तथा संघट्टन से सम्बन्धित मैग्माभवन

राकेश चन्द्रा, राजीव उपाध्याय एवं अंशु कुमार सिन्हा

श्योक सन्धिस्थल ज्वालामुखीय-वितलीय (प्लूटोनिक) शैल समुच्चयों के सुस्पष्ट सेटों द्वारा निरूपित हैं। श्योक ज्वालामुखी शैलों के उच्च-मैग्नीशियम के थोलीआइटी बेसाल्ट तथा कैल्क क्षारीय ऐन्डेज़ाइट में अपक्षय मण्डल के रासायनिक चिहन हैं। थोलीआइटी बेसाल्ट के दुर्लभ खनिज तत्व आंकड़ों से आद्य एन-एम.ओ.आर.बी. तथा ई.-एम.ओ.आर.बी. के बीच रासायनिक बन्धुता प्रस्तावित हुई है।

बहरहाल,कैल्क-क्षारी ऐन्डेजाइट ई-एम.ओ.आर.वी. तथा ओ.आई.बी. के बेसाल्ट की संक्रमी प्रकृति से सादृश्य प्रदर्शित करता है। भूरासायनिक आंकड़े तथा क्षेत्रीय विवर्तनिक सेटिंग उत्तरी लद्दाख के श्योक ज्वालामुखी शैल तथा कोहिस्तान के चाल्ट ज्वालामुखी शैलों के बीच गहन समरूपता को प्रस्तावित करती है।

तिरित् ग्रेनाइटाभ के हल्के विरूपित ट्रॉन्डझेमाइट-टोनेलाइट-ग्रेनोडायोराइट मिश्र प्लूटोन हैं, जो श्योक सन्धिस्थल मेलांज के दक्षिण में स्थित हैं। ये ग्रेनाइटाभ उपक्षारीय, आई. प्ररूपी हैं तथा ज्वालामुखीय चाप रासायनिक अवशेषों द्वारा निरूपित हैं। तिरित ग्रेनाइटाभों की क्षेत्रीय विवर्तनिक सेटिंग उपस्थिति की प्रकृति तथा संघट्टन उत्तरी कोहिस्तान (गिन्डाई, माटुम डैस एवं नोमाल प्लूटोन) की वितलीय (प्लूटोनिक) संजातियों के समतुल्य हैं।

पूर्वी कराकोरम महास्कन्ध में क्वार्ट्ज़ मोन्ज़ोनाइट-टोनेलाइट-ग्रेनोडायोराइट एवं ग्रेनाइट की प्रमुखता है। उपक्षारीय से कैल्क-क्षारीय के बीच कराकोरम महास्कन्ध ज्वालामुखीय चाप एवं सहसंघट्टन के रासायनिक अवशेषों से युक्त 'आई' एवं 'एस' दोनों ही प्ररूपों के ग्रेनाइटाभों द्वारा निर्मित है। दुर्लभ खनिज तत्व आंकड़ों से प्रस्तावित होता है कि पूर्वी कराकोरम के 'आई' प्ररूप के ग्रेनाइटाभ अपक्षय मण्डल के कैल्क-क्षारीय मैग्माभवन हैं। इसके विपरीत अधिकांश 'एस' प्ररूप के ग्रेनाइटाभ भूपटल से प्राप्त परएल्यूमिनस ग्रेनाइटाभ हैं। नवीनतम् रूबीडियम/स्ट्रॉन्शियम समग्र समस्थानिक शैल आयु निर्धारक आंकड़ों से संकेत मिलता है कि 8.3 ± 0.9 करोड़ वर्ष पूर्व के दौरान पूर्वी कराकोरम मण्डल में एक 'एस' प्ररूप की अन्तर्वेधी प्रावस्था सक्रिय थी। इन ग्रेनाइटाभों की सहसंघट्टन प्रकृति उत्तरी सास्ट प्लूटोन एवं करमबार प्लूटोन के समतुल्य है। इससे संकेत मिलता है कि 8.3 ± 0.9 करोड़ वर्ष पूर्व के दौरान कोहिस्तान-लद्दाख चाप तथा कराकोरम ब्लॉक के बीच संघट्टन सक्रिय था।

INTRODUCTION

The sequence of magmatic events as envisaged by the Indus Suture in Ladakh is believed to have started with a northward-directed intra-oceanic subduction of the Neo-Tethyan oceanic lithosphere in the Late Jurassic and Cretaceous (Honegger *et al.*, 1982). The Neo-Tethyan ocean probably closed along the Indus Suture around 50-60 Ma (Beck *et al.*, 1995; Sinha & Upadhyay, 1997; Upadhyay & Sinha, 1998).

The Ladakh block is in an intermediate position between the Indian Plate in the south and the Karakoram-Tibetan Plate in the north (Text-figure 1). To the west it is separated from the Kohistan arc by the Nanga Parbat syntaxis, to the east it is cut off from the Lhasa block by the Karakoram fault (Text-figures 1, 2). In the Ladakh block two important tectonic structures have been recognised and described by Gansser (1977) as the southern Indus Suture Zone (ISZ) and the northern Shyok Suture Zone (SSZ) (Northern Suture in Pakistan) (Text-figure 1). Located between the two sutures is the Trans-Himalayan Ladakh Batholith with mainly Cretaceous and Tertiary calc-alkaline intrusives which is subdivided from west to east into the Kohistan arc, the Ladakh magmatic arc and the Gangdese pluton of southern Tibet. The basaltic to andesitic Dras volcanics follow the Indus Suture and represent an island arc, which was active between the Late Jurassic and the Late Cretaceous (Honegger *et al.*, 1982; Dietrich *et al.*, 1983; Sharma, 1990). The Ladakh Batholith is unconformably overlain along its southern boundary by the molassic Indus Group of Miocene-Pliocene age.

The arc-batholith growth in Ladakh is discussed in terms of the Dras arc on the south side of the Ladakh Batholith (Schorer *et al.*, 1980; Dietrich *et al.*, 1983; Sharma, 1990) whereas in Kohistan it is related to the Chalt island arc volcanics which are on the north side of the batholith (Tahirkheli *et al.*, 1979; Coward *et al.*, 1986). Recently, it has been suggested that the Kohistan island arc was initiated offshore of Asia during the middle-Cretaceous and was sutured to Asia along the Northern Suture between 100 and 85 Ma (Petterson & Windley, 1985, 1991; Treloar *et al.*, 1996). So far very little is known about the subduction and closure of

PLATE 1 →

1a. Panoramic view of the Nubra-Shyok rivers confluence near the village of Tirit and Sumur. At the confluence point the Tirit Granitoids and associated rocks belong to Saltoro hills. The background snow covered peaks belong to the Ladakh Batholith, the foreground mountain belongs to Shyok Volcanics and Saltoro Formation as seen near the village of Diskit in Text-figure 2. View looking towards southwest.

1b. Outcrops of Shyok Volcanics as seen near the village of Diskit. View looking towards southwest.

1c. Panoramic view of the Nubra river valley showing the tectonoc juxtaposition of Shyok Ophiolitic Melange and Karakoram Batholith. View looking towards northeast as seen from the village of Charasa in Text-figure 2.

1a

1b

1c

PLATE 1

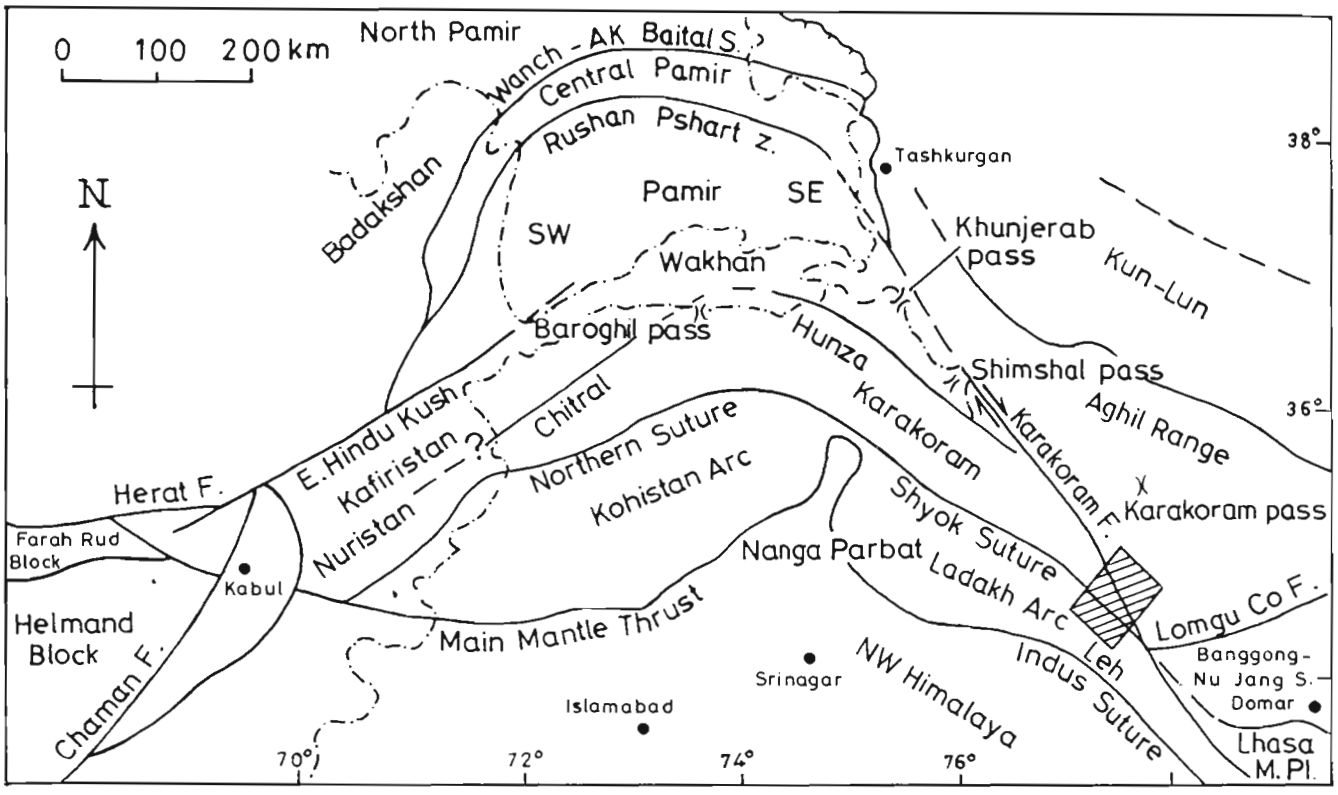

Text-figure 1–General tectonic map of Pamir, Karakoram, Kohistan and Ladakh showing the location of the Indus and Shyok Sutures together with the Kohistan and Ladakh arc terranes (modified after Gaetani (1997). Shaded box represent the area of study.

the Shyok Suture in northern Ladakh. Earlier, Rai (1982) presented evidence against subduction along the Shyok Suture. Brookfield and Reynolds (1981) and Reynolds *et al.* (1983) concluded that the Shyok Suture did not close until Miocene and therefore considered it as younger than the southern Indus Suture. However, Thakur and Mishra (1984) suggested that the Shyok Suture was the relict of a back-arc basin, whereas Srimal (1986) thought that the Shyok tectonic belt is one among several blocks that form a composite terrain between the northern margin of the Indian Plate and the southern margin of the Asian Plate and correlated the Shyok Suture with Jurassic-Early Cretaceous Bangong-Nujiang Suture in Tibet. Based on geological information from the poorly known Nubra-Shyok region it appears that there are major stratigraphic and structural differences along the Shyok Suture Zone exposed in northern Ladakh and Kohistan (Sinha & Upadhyay, 1997).

This paper deals primarily with the results of a recent study on the Shyok Suture and adjoining eastern Karakoram batholith exposed in the Shyok-Nubra valleys in northern Ladakh, which forms an accretionary complex immediately north of the Ladakh magmatic arc. We present new field observations together with regional geology, petrography, geochemical and geochronological data on magmatism. We also discuss these data to deduce tectonic setting and tectono-magmatic evolution of the Shyok Suture and eastern Karakoram Batholith . An attempt has also been made for regional correlation of presently investigated area with the geologically better known sections of northern Kohistan.

GEOLOGICAL SETTING

The rocks of the SSZ, trending northwest-southeast (Text-figures., 2, 3) across the Nubra-Shyok valleys, occur in a number of intensely deformed tectonic slices between the Ladakh Batholith to the southwest and Karakoram Batholith to the northeast (Text-figures 2,3, Plate 1 a, c). These tectonic slices comprise a variety of sedimentary, volcanic and plutonic rocks hence referred an accretionary complex (Sinha & Upadhyay, 1997). To the south, the lowermost imbricate of the Shyok Suture is built up by Late Jurassic to Early-middle Cretaceous Saltoro Formation (Upadhyay *et al.*, 1999). The Saltoro Formation is in tectonic contact along a steeply dipping thrust with the calc-alkaline volcanics and volcanoclastics of Khardung Formation of the ISZ (Text-figures 3, 4). The tectonic contact between Shyok Ophiolitic Melange and Karakoram Batholith mark the northern limit of the Shyok Suture (Text-figures 2, 3, 4, Plate 1c). Geological account of Shyok Suture has recently been given and discussed elsewhere (Rai, 1991; Upadhyay *et al.*, 1999). Apart from other rock types the Shyok Suture is represented by a variety of different sets of volcano-plutonic rock assemblages. For the purpose

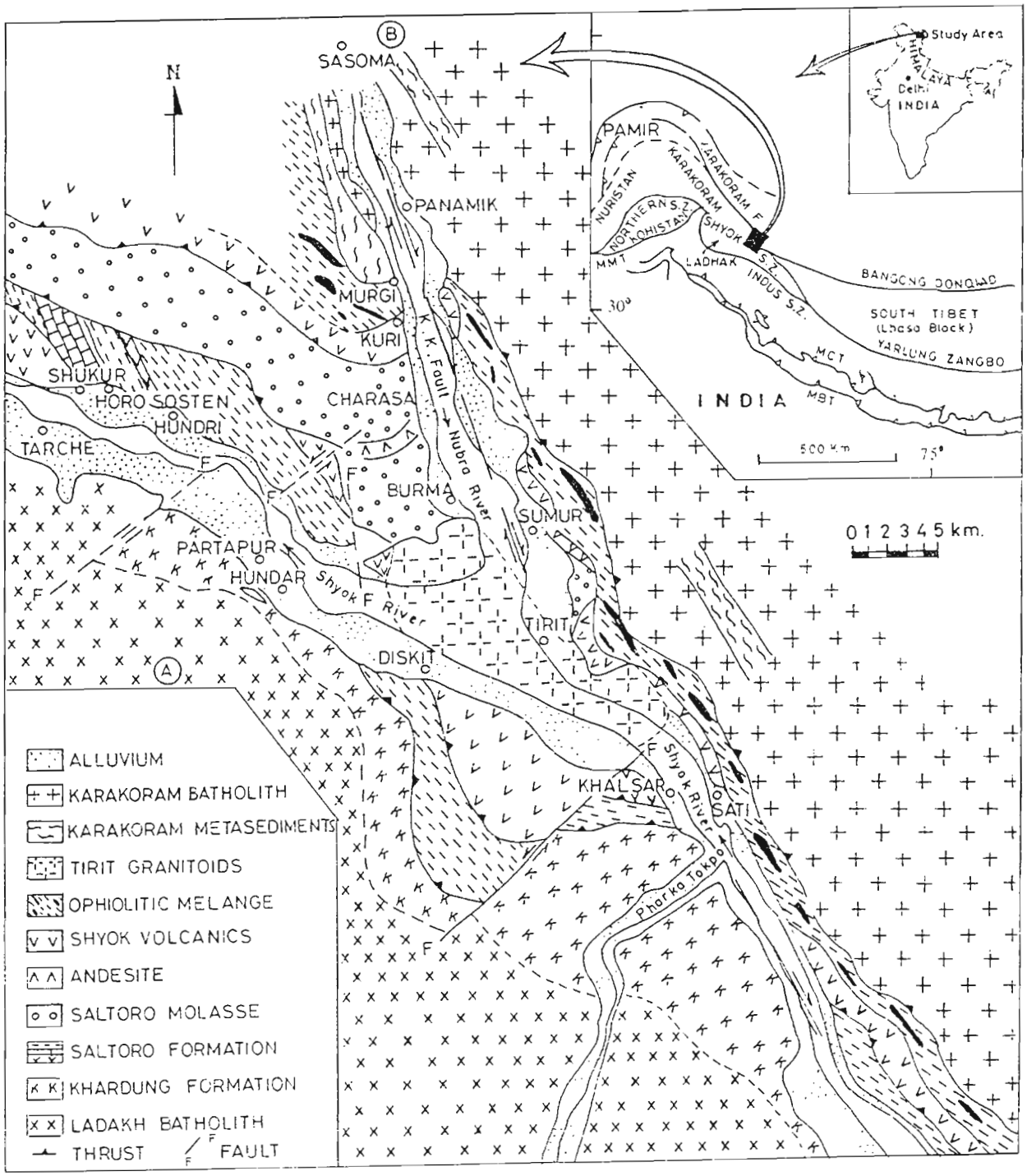

Text-figure 2–Geological map of the Shyok Suture Zone and eastern Karakoram in the Nubra-Shyok valley, northern Ladakh, India.

of present study, the occurrences of several Volcano-plutonic bodies have been grouped and discussed as: 1. Shyok Volcanics; 2. Tirit Granitoids; 3. Karakoram Batholith.

Shyok Volcanics

Under the heading of Shyok Volcanics we describe different occurrences of volcanics in the Nubra-Shyok valleys of which we do not know their original palaeogeographic position (Plate 1a, b). Sporadic outcrops occur below the Saltoro Formation (Upadhyay *et al.*, 1999) near Shukur (Text-figure 2). Southeast of Diskit the Saltoro Formation is tectonically overlain along a steeply dipping thrust by chlorite schists, basic volcanics and cherts of the Shyok Volcanics (Text-figures 2, 3). West of the Karakoram Fault they also

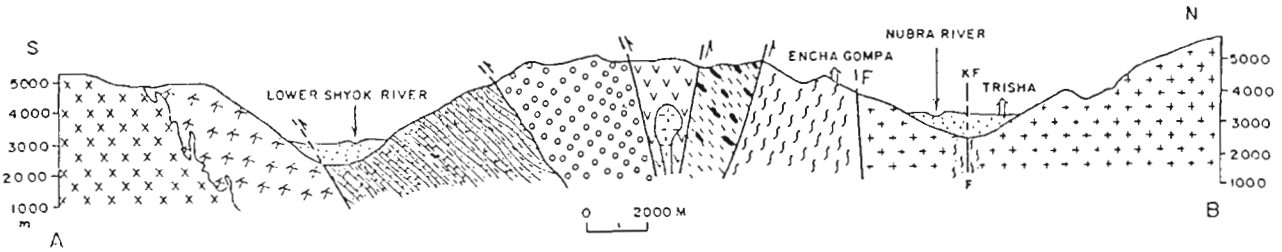

Text-figure 3–Geological cross-section along line A-B on Text-figure 2.

occur tectonically sandwiched between the underlying Saltoro Molasse and Ophiolitic Melange, above. East of the Karakoram Fault, they crop out between the villages of Panamik and Tirit and near confluence of the Nubra-Shyok rivers (Plate 1a). Rai (1991) estimated that they are up to 4 km thick, consisting of a heterogeneous sequence of basalts and andesites with ignimbrites. Individual flows could not be traced across the inaccessible outcrops. At several places, the Shyok Volcanics are intruded by granodiorite, tonalite to gabbrodiorite plutonic bodies known as Tirit Granitoids (Text-figures 2, 3, 4).

Compositionally, the Shyok Volcanics range from basalt, basaltic andesite to andesite. The basaltic rocks exposed near the village of Shukur and Sati bridge are fine-to medium-grained, massive and highly fractured, with rare vesicles. These rocks are essentially made up of plagioclase, hornblende and augite whereas olivine is present in accessory amount. Plagioclase and augite occurs as minute radiating laths and showing sub-ophitic texture. The basaltic andesites exposed near the village of Trisha and Tegar are medium-grained, agglomeratic and ophitic in texture; vesicles are well developed and vary from a few mm to 1 cm in diameter, which are filled with calcite, zeolite and chlorite. The basaltic andesites are strongly epidotised. These rocks are also cut by hydro-

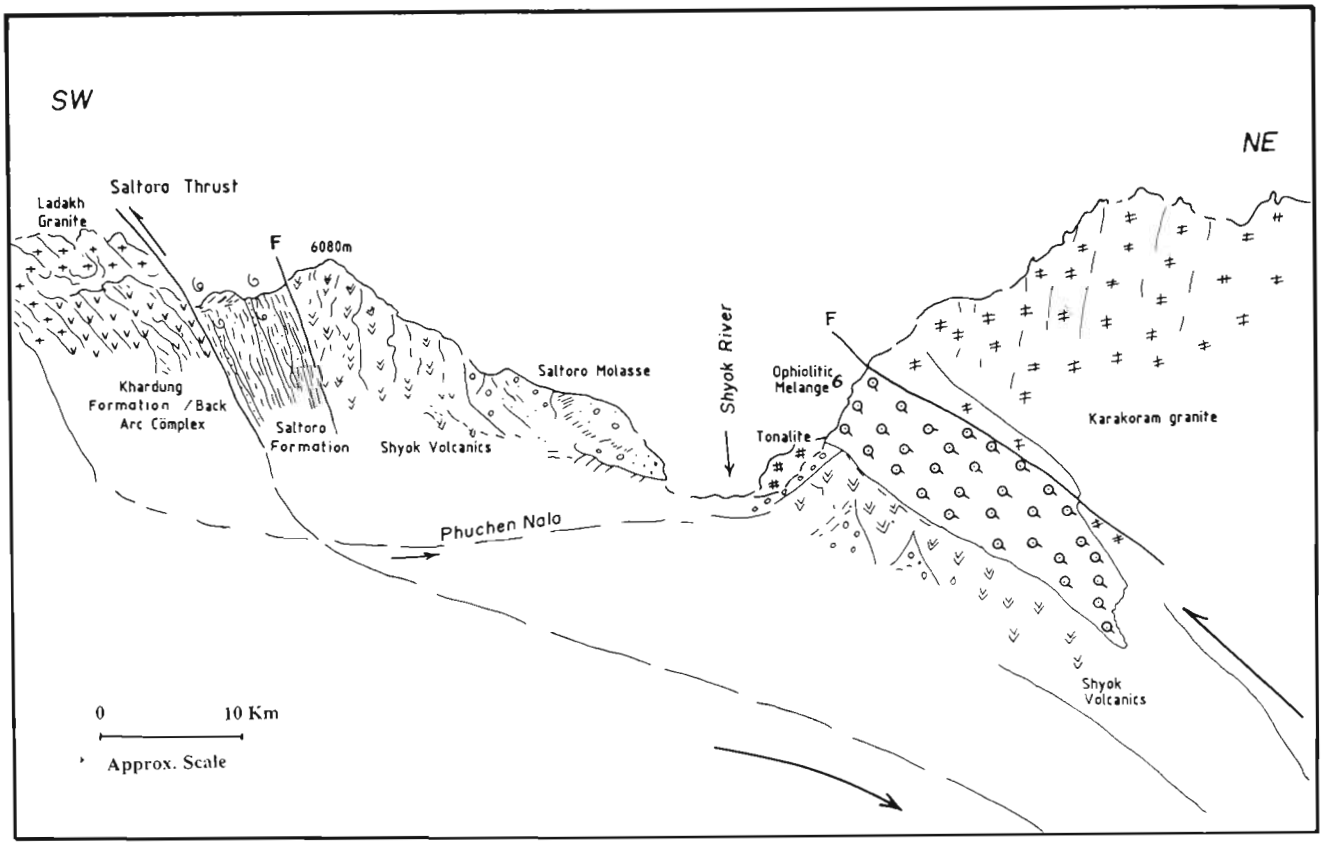

Text-figure 4–Field sketch cross-section across the Shyok Suture Zone near the village of Khalsar.

thermal veins rich in sulphide mineralisation, mainly chalcopyrite and flaky hematite. These rocks are made up of plagioclase, hornblende, biotite and quartz. Sphene, zircon, epidote and chlorite present as secondary minerals. The twinned plagioclase crystals are intensively altered. The pyroxene and hornblende is also present in the fine-grained groundmass which is dominated by plagioclase microlites. The hornblende crystals show two distinct sets of cleavage. Flakes of biotite represent characteristic diachroism from light brown to deep brown. Black iron ore, opaques and chlorite are also present. The andesites show well developed laths of plagioclase phenocrysts showing porphyritic texture. Plagioclase laths are zoned, clouded, twinned and are embedded in fine–grained, epidotized groundmass. Augite occurs as prismatic crystals. The groundmass is composed of microphenocrysts and microlites of augite and plagioclase. Hornblende show typical bluish-green colour and exhibiting simple twinning.

Geochemistry of Shyok Volcanics

A total of 43 samples of Shyok Volcanics were analyzed and are presented in Table 1. Major, trace and rare earth elements (REE) were determined by X-ray fluorescence spectrometry (Siemens SRS 3000) and inductively coupled plasma-atomic emission spectrometry (Jobin Yvon JY-70 plus) at the Geochemical Laboratory of the Wadia Institute of Himalayan Geology, Dehradun. International rock geo-standards BHVO-1, MBH and DGH were used for calibration. Major elements have been used to determine the CIPW norms.

The Shyok Volcanics show a wide variation in their geochemical ranges. On the basis of sampling from different localities, the analysed samples have been classified and discussed as volcanic rocks from Shukur village, Tegar village and Sati bridge. According to chemical classification proposed by Peccerillo and Taylor (1976), Winchester and Flyod (1977) and Cox *et al.* (1979) the Shyok Volcanics ranges from basalts,

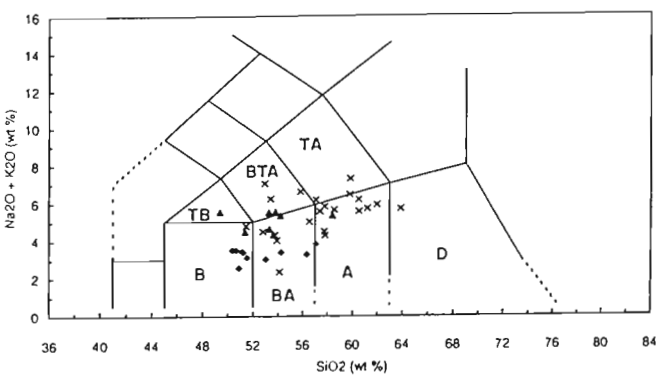

Text-figure 5–$Na_2O + K_2O$ versus SiO_2 chemical classification diagram for Shyok Volcanics (plotted on the diagram after Cox *et al.*, 1979). **B** = basalt; **BA** = basaltic andesite; **A** = andesite; **D** = dacite; **TB** = trachy basalt; **BTA** = basaltic trachy andesite; **TA** = trachy andesite. Filled rhombus = Shukur volcanics; cross = Tegar Volcanics; filled triangles = Sati bridge volcanics.

basaltic - andesite to andesites. The total alkali silica (TAS) ($Na_2O + K_2O$ % versus SiO_2%) chemical classification scheme (Cox *et al.*, 1979) show that the Shyok Volcanics are basalt, trachy-basalt, basaltic-andesite, basaltic-trachy-andesite, andesite, trachy-andesite and dacite (Table 1; Text-figure 5).

The basalt samples have a range of SiO_2 content from 47.16 to 52.57%. Similarly basaltic-andesite with 52.97 to 57.63 % and andesites 58.07 to 62.1 % (Table 1). The systematic increase in SiO_2 from basalt to andesite through basaltic - andesite suggests that no compositional gap seems to exist between the geochemical characters of Shyok Volcanics which may represent a common parent magma. All the samples are characterised by low values of TiO_2 wt% which ranges from 0.47 to 1.48%, and comparable with island arc volcanics. These volcanics are moderately enriched in Al_2O_3 (13.96 to 17.58%), MgO (4.9 to 12.01%) and total iron (Fe_2O_3) (4.15 to 11.27%). It is evident from petrography that rocks of the Shyok Volcanics have suffered post magmatic secondary alterations and therefore have very high values of LOI (Table 1). This suggests that these rocks must have induced the effect of element mobilization, particularly the alkali elements which are highly mobile and showing a wide range of their concentrations. In most samples the Na_2O content is generally higher than K_2O values and ranges from 0.44 to 5.88%. The K_2O values ranges from 0.01 to 4.12 %. Some samples are exceptionally enriched in their soda content (> 4%). This may be due to spilitization of the volcanic rocks. The trace element data (Table 1) of these volcanics suggest that radioactive elements, such as Rb, Th and U contents are very low. These elements are generally associated with continental crust. The Shyok Volcanics have very low values of Nb (0.1 to 26 ppm), Pb (5 to 24 ppm) and Ga (13 to 22 ppm). The depletion of Nb is generally associated with calc-alkaline subduction related magmatism. The Zn, Cu, Ni, Cr are moderately enriched in basalts and their concentration decreases toward andesite samples. All the samples are moderately enriched in Ba, Ni, Cr and Sr elements. Higher Sr content like 605 ppm suggest either the fractionation of calc-plagioclase or the hydrothermal enrichment.

In major oxide versus MgO% plots (Text-figure 6) the concentration of SiO_2, Al_2O_3, Na_2O and K_2O decreases with increasing value of MgO%. Whereas, total iron Fe_2O_3(t), MnO and TiO_2 shows a positive correlation with increasing value of MgO%. All the samples are depleted in TiO_2 except for high Mg volcanics of Shukur village. The total iron and TiO_2 variation plots for Shukur village volcanics show a tholeiitic to transitional tholeiitic/calc-alkaline nature of magma. The samples from Tegar village and Sati bridge represent calc-alkaline trend and a positive correlation with MgO% (Table 1). The A ($Na_2O + K_2O$) - F (FeO^*) – M (MgO) diagram further confirm the tholeiitic and calc-alkaline characters for Shyok Volcanics.

Table 1—Geochemical data for Shyok Volcanics

Locality	Shukur village							
S.No.	SV R59	SV R58	SV R66	SV R62	SV R63	SV R60	SV R65	SV R64
Rock Type	B	B	B	B	B	B	B	B
Major Oxides (wt%)								
SiO_2	47.16	47.87	48.27	48.64	49.1	49.16	49.23	52.22
TiO_2	1.25	0.56	0.7	0.64	0.69	0.47	0.77	0.78
Al_2O_3	16.12	14.08	14.61	15.49	14.81	14.59	14.77	15.05
FeO(t)	14.31	10.99	11.06	10.84	11.93	9.12	11.81	10.39
MnO	0.16	0.19	0.2	0.22	0.18	0.19	0.2	0.2
MgO	8.77	10.62	9.44	7.53	8.26	10.11	8.92	10.65
CaO	2.54	8.35	9.14	10.22	8.87	9.59	5.47	4.58
Na_2O	1.85	1.66	3.2	3.131	2.23	1.74	2.5	2.85
K_2O	1.26	0.74	0.14	0.22	0.95	1.22	0.28	0.41
P_2O_5	0.09	0.07	0.18	0.14	0.12	0.15	0.12	0.15
LOI	6.43	3.73	3.8	4.6	3.8	3.7	5.59	3.75
Total	99.94	98.86	100.74	101.671	100.94	100.04	99.66	101.03
Trace Elements (ppm)								
Ba	n.d	261.6	764.1	195.4	296.8	230.9	154.4	n.d
Cr	156	430	147	126	248	233	86	132
Ni	77	242	24	18	109	57	27	144
Cu	137	109	122	33	148	27	567	1756
Zn	165	102	91	88	104	94	104	103
Ga	19	13	18	16	18	15	17	16
Pb	8	6	11	7	12	47	13	10
Th	1.24	1.32	67	1.6	0.99	3.57	3.15	2.01
Rb	42	28	n.d	10	19	41	14	20
U	0.86	1.06	0.53	0.96	0.55	1.65	0.85	1.05
Sr	90	119	530	810	225	164	556	351
Y	23	15	18	17	19	20	18	19
Zr	83	35	73	76	58	67	80	69
Nb	5	4	1	1	2	1	1	1
Rare Earth Elements (ppm)								
La	n.d	5.2	15.6	13.5	17.5	17.3	n.d	n.d
Ce	n.d	8.2	29.8	21.1	30.9	28.7	n.d	n.d
Nd	n.d	5.5	15.5	12.1	15.8	14.3	n.d	n.d
Sm	n.d	1.81	4.15	3.22	4.18	3.48	n.d	n.d
Eu	n.d	0.519	1.01	0.975	1.17	1.06	n.d	n.d
Gd	n.d	1.73	3.66	2.9	3.86	2.89	n.d	n.d
Dy	n.d	2.01	3.38	2.88	3.48	2.79	n.d	n.d
Er	n.d	1.3	2.13	1.78	2.04	1.69	n.d	n.d
Yb	n.d	1.2	1.85	1.66	2.01	1.69	n.d	n.d
Lu	n.d	0.2	0.293	0.252	0.31	0.276	n.d	n.d
CIPW Norm								
q	7.71	-	-	-	-	-	4.06	4.58
or	7.45	4.37	0.83	1.3	5.61	7.21	1.65	2.42
ab	16.65	14.05	27.08	26.49	18.27	14.72	21.35	24.12
an	12.01	28.78	25.09	27.57	27.6	28.4	26.35	21.74
hy	34.15	31.35	9.97	9.45	25.03	23.93	32.92	35.82
mt	5.6	4.29	4.32	4.23	4.67	3.57	4.61	4.06
il	2.37	1.06	1.33	1.22	1.31	0.89	1.46	1.48
ap	0.21	0.16	0.42	0.32	0.28	0.35	0.28	0.35
di	-	9.8	15.38	18.02	12.67	14.59	-	-
C	7.31	-	-	-	-	-	0.7	1.95
ol	-	0.45	11.7	7.67	0.22	2.01	-	-
ne	-	-	-	-	-	-	-	-
Plagioclase	An43	An67	An48	An51	An59	An66	An55	An47

Contd.

Locality	Shukur village			Sati bridge				
S.No.	SV R61	SV R67	SV R78	SB R33	SB R34	SB R38	SB R31	SB R37
Rock Type	BA	BA	A	B	B	B	B	B
Major Oxides (wt%)								
SiO_2	53.18	54.37	58.54	48.95	49.29	50.75	51.52	52.17
TiO_2	0.77	0.93	0.61	0.96	1.11	0.85	1.07	0.97
Al_2O_3	15.24	15.14	16.22	16.49	14.63	15.56	14.62	15.27
Fe(t)	9.59	10.03	5.58	10.01	9.58	8.36	9.12	8.6
MnO	0.16	0.18	0.1	0.15	0.14	0.12	0.13	0.14
MgO	6.77	10.07	5.11	8.3	10.31	8.52	9.66	8.24
CaO	4.78	3.56	5.28	9.55	7.26	6.95	6.72	6.84
Na_2O	3.16	3.08	2.72	0.44	3.1	2.95	3.14	3.43
K_2O	0.39	0.05	2.65	5.03	1.17	1.14	1.31	1.92
P_2O_5	0.12	0.12	0.18	0.27	0.33	0.25	0.28	0.28
LOI	6.34	3.32	4.8	2.3	3.95	4.69	3.26	2.95
Total	100.5	100.85	101.79	102.45	100.87	100.14	100.83	100.81
Trace Elements (ppm)								
Ba	112.6	120.5	n.d	n.d	n.d	574.3	403.8	502.9
Cr	91	32	164	262	256	164	295	203
Ni	32	20	25	96	120	217	146	81
Cu	28	201	24	6	35	68	66	47
Zn	107	95	81	99	85	76	83	86
Ga	16	16	18	15	16	14	18	17
Pb	12	5	13	11	24	5	135	9
Th	1.41	1.6	3.23	3.9	4.97	5.8	6.07	4.31
Rb	15	7	88	152	39	53	47	71
U	0.98	0.64	2.54	4.19	1.56	1.9	1.74	2.24
Sr	119	154	220	176	477	5.1	389	380
Y	24	24	13	17	23	24	22	22
Zr	68	87	120	121	136	124	139	149
Nb	4	4	6	7	7	8	7	8
Rare Earth Elements (ppm)								
La	n.d	8.89	n.d	n.d	n.d	18.9	22.2	18.1
Ce	n.d	16.05	n.d	n.d	n.d	32.8	37.45	32.2
Nd	n.d	10.94	n.d	n.d	n.d	18.3	21.7	17.4
Sm	n.d	3.85	n.d	n.d	n.d	4.41	5.04	4.07
Eu	n.d	1.06	n.d	n.d	n.d	1.33	1.4	1.22
Gd	n.d	4.03	n.d	n.d	n.d	4.08	4.04	3.48
Dy	n.d	4.69	n.d	n.d	n.d	3.9	3.48	3.39
Er	n.d	2.86	n.d	n.d	n.d	1.95	1.59	1.69
Yb	n.d	2.4	n.d	n.d	n.d	1.91	1.63	1.61
Lu	n.d	0.349	n.d	n.d	n.d	0.284	0.248	0.237
CIPW Norm								
q	9.46	10.02	12.06	-	-	0.64	-	-
or	2.3	0.3	15.66	29.73	6.91	6.74	7.74	11.35
ab	26.74	25.06	23.03	3.73	26.23	24.96	26.57	29.02
an	22.93	16.88	24.22	28.17	22.55	25.85	21.93	20.6
hy	25.32	33.75	17.38	4.28	13.82	25.57	23.99	15.97
mt	3.74	3.91	2.29	3.91	3.74	3.26	3.57	3.36
il	1.46	1.77	1.16	1.82	2.11	1.61	2.03	1.84
ap	0.28	0.28	0.42	0.63	0.76	0.58	0.65	0.65
di	-	-	0.64	14.06	9.05	5.61	7.66	9.23
C	1.22	3.83	-	-	-	-	-	-
ol	-	-	-	13.09	11.03	-	2.76	5.21
ne	-	-	-	-	-	-	-	-
Plagioclase	An46	An39	An51	An88	An46	An51	An45	An42

Contd.

Locality	Sati Bridge				Tegar village			
S.No.	SB R36	SB R35	SB R32	SB R39	TV R74	DB R83	SB R82	CH R75
Rock Type	B	BA	BA	B	B	B	B	BA
Major Oxides (wt%)								
SiO_2	52.3	52.57	57.49	50.71	50.71	51.01	51.94	52.97
TiO_2	0.64	0.88	0.88	0.84	0.82	1.08	0.92	0.96
Al_2O_3	15.26	16.98	16.59	15.46	15.48	15.54	17.58	15.55
FeO(t)	8.59	8.64	6.66	8.31	7.6	8.41	6.67	6.96
MnO	0.15	0.12	0.09	0.12	0.06	0.11	0.07	0.08
MgO	8.41	7.02	5.77	8.49	12.01	10.59	8.3	9.64
CaO	6.31	7.66	6.13	6.92	3.04	8.32	6.17	2.98
Na_2O	3.44	1.31	3.22	2.92	4.39	3.76	3.44	5.13
K_2O	1.69	4.12	2	1.14	2.33	0.96	2.59	1.11
P_2O_5	0.27	0.27	0.28	0.25	0.16	0.26	0.23	0.19
LOI	2.89	1.99	2.05	4.97	3.2	2.78	3.78	4.7
Total	99.95	101.56	101.16	100.13	99.8	102.82	101.69	100.27
Trace Elements (ppm)								
Ba	n.d	n.d	n.d	176	313.7	n.d	n.d	n.d
Cr	209	215	155	161	159	254	146	170
Ni	84	72	34	43	124	131	58	122
Cu	10	5	3	5	13	5	6	78
Zn	99	71	58	41	27	34	31	47
Ga	19	16	17	18	19	21	18	18
Pb	7	9	7	11	10	7	5	13
Th	5.15	6.52	10.23	3.64	4.45	4.04	3.02	4.04
Rb	62	132	67	49	58	19	67	26
U	2.08	3.5	2.13	1.86	1.97	1.14	2.19	1.61
Sr	248	159	402	240	339	477	320	260
Y	22	17	21	20	18	21	20	17
Zr	154	142	184	160	182	142	148	191
Nb	8	7	9	6	6	7	7	5
Rare Earth Elements (ppm)								
La	n.d	n.d	n.d	n.d	15.7	n.d	n.d	n.d
Ce	n.d	n.d	n.d	n.d	32.6	n.d	n.d	n.d
Nd	n.d	n.d	n.d	n.d	16	n.d	n.d	n.d
Sm	n.d	n.d	n.d	n.d	4.43	n.d	n.d	n.d
Eu	n.d	n.d	n.d	n.d	0.848	n.d	n.d	n.d
Gd	n.d	n.d	n.d	n.d	3.67	n.d	n.d	n.d
Dy	n.d	n.d	n.d	n.d	3.27	n.d	n.d	n.d
Er	n.d	n.d	n.d	n.d	1.95	n.d	n.d	n.d
Yb	n.d	n.d	n.d	n.d	1.36	n.d	n.d	n.d
Lu	n.d	n.d	n.d	n.d	0.206	n.d	n.d	n.d
CIPW Norm								
q	-	1.48	8.56	0.9	-	-	-	-
or	9.99	24.35	11.82	6.74	13.77	5.67	15.31	6.56
ab	29.11	11.08	27.25	24.71	36.75	31.82	29.11	43.41
an	21.21	28.29	24.91	25.71	14.04	22.69	24.88	13.54
hy	21.57	21.65	18.21	25.47	-	2.74	8.91	16.13
mt	3.35	3.38	2.6	3.25	2.9	3.29	2.61	2.71
il	1.79	1.67	1.67	1.6	1.56	2.05	1.75	1.82
ap	0.63	0.63	0.65	0.58	0.37	0.6	0.53	0.44
di	6.68	6.41	2.95	5.6	-	13.5	3.37	-
C	-	-	-	-	0.59	-	-	0.95
ol	2.41	-	-	-	25.8	17.11	10.96	9.48
ne	-	-	-	-	0.22	-	-	-
Plagioclase	An42	An72	An48	An51	An28	An42	An46	An24

Contd.

Locality	Tegar village							
S.No.	DV R84	SB R41	TV R69	SB R40	TV R72	CH R76	TV R68	CHK R81
Rock Type	BA	BA	BA	BA	BA	BA	BA	BA
Major Oxides (wt%)								
SiO_2	52.98	53.38	54.65	54.9	55.27	56.44	56.84	56.97
TiO_2	0.96	0.72	0.51	0.47	1.19	1.48	0.85	1.14
Al_2O_3	15.77	13.96	14.18	17.08	15.37	16.18	14.76	16.61
FeO(t)	9.9	7.68	11.27	10.39	9.44	8.59	7.62	6.13
MnO	0.18	0.16	0.12	0.1	0.04	0.1	0.11	0.11
MgO	7.92	8.5	5.31	4.9	6.58	5.55	7.12	7.16
CaO	8.94	11.28	5.42	12.07	3.81	7.05	6	6.3
Na_2O	2.21	3.8	4.02	1.37	4.36	3.34	4.53	3.6
K_2O	2.29	0.17	0.01	1.01	0.97	1.64	1.18	1.73
P_2O_5	0.2	0.16	0.17	0.2	0.19	0.3	0.15	0.34
LOI	3.35	1.31	4.7	1.25	2.31	2.3	2.7	2.71
Total	104.7	101.12	100.36	103.74	99.53	102.97	101.86	102.8
Trace Elements(ppm)								
Ba	n.d	266.5	81.06	299.7	187.1	234	n.d	435
Cr	156	234	88	230	188	139	168	209
Ni	30	28	29	29	98	19	46	101.4
Cu	64	57	7	0	35	49	13	20.3
Zn	112	49	90	15	18	52	37	62.1
Ga	17	15	19	40	19	20	17	18.5
Pb	9	119	10	11	4	6	8	7
Th	4.5	2.44	1.77	1.24	2.54	5.86	0.48	3.9
Rb	84	5	6	31	33	40	60	35
U	2.75	0.9	0.29	1.77	1.37	1.62	2.07	1
Sr	420	495	114	495	295	503	207	605
Y	26	28	32	30	21	29	24	19
Zr	111	95	151	96	142	190	102	220
Nb	4	6	12	4	4	8	5	14
Rare Earth Elements (ppm)								
La	n.d	n.d	21.1	33.2	16.5	21.8	n.d	n.d
Ce	n.d	n.d	53	52.7	29	39.8	n.d	n.d
Nd	n.d	n.d	28.9	21.9	18.06	21.1	n.d	n.d
Sm	n.d	n.d	7.69	5.29	4.54	5.44	n.d	n.d
Eu	n.d	n.d	1.19	1.37	1.03	1.65	n.d	n.d
Gd	n.d	n.d	6.65	4.7	3.83	5.04	n.d	n.d
Dy	n.d	n.d	6.36	4.81	3.5	4.64	n.d	n.d
Er	n.d	n.d	3.79	2.39	1.98	2.45	n.d	n.d
Yb	n.d	n.d	3.28	2.32	1.36	1.89	n.d	n.d
Lu	n.d	n.d	0.482	0.331	0.215	0.289	n.d	n.d
CIPW Norm								
q	0.71	-	8.52	10.64	5.39	7.26	2.71	5.29
or	13.53	1	0.06	5.97	5.73	9.69	6.97	10.22
ab	18.7	32.15	34.02	11.59	36.89	28.26	38.33	30.46
an	26.35	20.53	20.62	37.47	17.66	24.31	16.46	24.06
hy	21.27	9.81	21.63	13.31	23.78	16.62	19.31	20.29
mt	3.87	3	4.35	4.06	3.68	3.35	2.9	2.39
il	1.82	1.37	0.97	0.89	2.26	2.81	1.61	2.17
ap	0.46	0.37	03.9	0.46	0.44	0.7	0.35	0.79
di	13.46	27.52	4.24	17.32	-	7.02	9.9	3.96
C	-	-	-	-	0.68	-	-	-
ol	13.46	3.48	-	-	-	-	-	-
ne	-	-	-	-	-	-	-	-
Plagioclase	An58	An39	An38	An76	An32	An46	An30	An44

Contd.

Locality	Tegar village							
S.No.	TV R70	SB R30	TV R71	CHK R80	SB R42	SB R29	SB R45	SB R43
Rock Type	BA	BA	BA	A	A	A	A	A
Major Oxides (wt%)								
SiO_2	57.4	57.51	57.63	58.07	58.53	6.04	60.37	60.51
TiO_2	1.07	0.85	1.03	1.03	0.66	0.72	0.68	0.72
Al_2O_3	14.93	15.93	15.21	16.79	16.26	15.94	15.52	14.75
FeO(t)	7.81	8.82	6.87	6.29	5.99	5.4	4.76	6.43
MnO	0.05	0.25	0.05	0.09	0.06	0.1	0.07	0.11
MgO	7.14	5.89	7.62	6.33	5.52	5.41	5.13	5.36
CaO	7.13	6.02	5	5.67	3.5	5.78	4.92	7.29
Na_2O	3.1	4.59	3.67	3.14	3.75	5.88	4.75	4.59
K_2O	1.35	1.6	1.86	2.73	1.68	1.41	1.93	1.91
P_2O_5	0.2	0.19	0.2	0.26	0.25	0-.25	0.28	0.18
LOI	2.78	2.08	2.5	2.05	4.02	1.91	2.78	1.05
Total	102.96	103.73	101.64	102.45	100.22	102.84	101.19	102.9
Trace Elements (ppm)								
Ba	124.6	230.2	176.9	735	n.d	232.1	n.d	n.d
Cr	252	142	188	190	157	182	n.d	268
Ni	65	25	71	109.6	28	18	30	59
Cu	7	12	188	18.7	30	5	47	8
Zn	23	86	25	74.2	39	17	45	68
Ga	18	19	16	19.2	17	18	18	17
Pb	9	13	6	5	13	13	9	17
Th	4.72	6.32	5.44	1.6	7.64	11.97	2.24	6.85
Rb	48	75	74	62	77	65	78	65
U	1.83	2.36	2.28	1.6	2.22	2.15	2.58	2.22
Sr	553	328	444	682	285	307	413	398
Y	23	44	19	20	17	47	25	21
Zr	129	172	127	189	192	225	111	169
Nb	6	15	5	11	7	26	4	6
Rare Earth Elements (ppm)								
La	15.8	n.d	9.1	n.d	n.d	27.8	n.d	n.d
Ce	29.7	n.d	16.5	n.d	n.d	54.3	n.d	n.d
Nd	15.9	n.d	9.7	n.d	n.d	28.1	n.d	n.d
Sm	4.53	n.d	2.84	n.d	n.d	7.92	n.d	n.d
Eu	1.43	n.d	0.727	n.d	n.d	1.16	n.d	n.d
Gd	4.3	n.d	2.63	n.d	n.d	7.28	n.d	n.d
Dy	4.03	n.d	2.94	n.d	n.d	8.88	n.d	n.d
Er	2.03	n.d	1.63	n.d	n.d	5.15	n.d	n.d
Yb	1.44	n.d	1.14	n.d	n.d	6.08	n.d	n.d
Lu	0.194	n.d	0.1496	n.d	n.d	0.816	n.d	n.d
CIPW Norm								
q	8.53	2.26	6.17	6.98	12.86	1.78	6.87	5.5
or	7.98	9.46	10.99	16.13	9.93	8.33	11.41	11.29
ab	26.23	38.84	31.05	26.57	31.39	49.76	40.19	38.84
an	22.84	18.14	19.54	23.66	15.73	12.94	15.33	14
hy	19.48	18.34	22.62	19.36	18.65	12.37	15.76	10.56
mt	3.04	3.33	2.68	2.45	2.33	2.1	1.86	2.51
il	2.03	1.61	1.96	1.96	1.25	1.37	1.29	1.37
ap	0.46	0.44	0.46	0.6	0.58	0.58	0.65	0.42
di	9	8.5	3.16	2.22	-	11.29	5.86	16.89
C	-	-	-	-	2.46	-	-	-
ol	-	-	-	-	-	-	-	-
ne	-	-	-	-	-	-	-	-
Plagioclase	An47	An32	An39	An47	An33	An21	An28	An27

Contd.

Locality	Tegar village		
S.No.	SB R44	TV R73	SV R77
Rock Type	A	A	A
Major Oxides (wt%)			
SiO_2	60.57	60.72	62.1
TiO_2	0.68	0.62	0.52
Al_2O_3	15.56	14.7	15.64
FeO(t)	5.28	8.29	4.15
MnO	0.09	0.05	0.09
MgO	6.12	5.16	4.86
CaO	5.96	3.34	4.64
Na_2O	4.85	4.19	4.17
K_2O	1.33	1.57	1.35
P_2O_5	0.17	0.15	0.17
LOI	1.45	2.78	3.2
Total	102.06	101.57	100.89
Trace Elements (ppm)			
Ba	483.4	n.d	296.4
Cr	244	130	220
Ni	52	84	37
Cu	5	245	11
Zn	57	22	73
Ga	17	18	19
Pb	13	8	10
Th	5.96	1.62	8.16
Rb	42	73	43
U	1.77	2.25	1.57
Sr	392	300	460
Y	16	17	12
Zr	137	134	129
Nb	5	4	5
Rare Earth Elements (ppm)			
La	21.7	n.d	19.5
Ce	34.2	n.d	35.6
Nd	19.3	n.d	15.1
Sm	4.24	n.d	2.95
Eu	1.13	n.d	0.868
Gd	3.12	n.d	2.33
Dy	2.61	n.d	1.77
Er	1.33	n.d	0.673
Yb	1.01	n.d	0.868
Lu	0.169	n.d	0.144
CIPW Norm			
q	6.46	12.63	14.85
or	7.86	9.28	7.98
ab	41.04	35.45	35.29
an	16.76	15.59	19.97
hy	15.01	20.07	14.74
mt	2.06	3.23	1.62
il	1.29	1018	0.99
ap	0.39	0.35	0.39
di	9.39	-	1.55
C	-	0.39	-
ol	-	-	-
ne	-	-	-
Plagioclase	An29	An31	An36

The trace element versus MgO% variation diagram show consistent correlation between trace elements (Text-figure 7) except Ba and Sr. The scattering of Sr/CaO is mainly attributed to post crystallization alteration or metamorphism. A negative correlation can be seen in Rb, Zr, Ga, Th and U elements. The concentration of these elements decreases systematically with the increasing value of MgO%. A positive correlation can also be inferred for Ni versus MgO%. The total iron and TiO_2 bivariation plots depicts that there is a compositional gap between the high Mg tholeiitic basalt of Shukur village and low Mg calc-alkaline rocks of Tegar village and Sati bridge. Similar geochemical gaps are also present in Ni, Cr, Y and Nb. Hence, it is inferred that these volcanics are either representing two different magma types or the effect of secondary alterations.

Nineteen representative samples were analyzed for Rare Earth Elements (REE) (Table 1). The geochemical results are compared with the Normal Mid Oceanic Ridge Basalt (N - MORB), Enriched Mid Oceanic Ridge Basalt (E - MORB), and Oceanic Island Basalt (OIB) (Sun and Mc Donough, 1989). It is observed that some of the samples are moderately enriched in all the REE, whereas, few samples show depletion which is similar to those found in N- and E-MORB. Samples from Shukur village (Table 1; Text-figure 8) are characterised by depletion in all the REE $\{(Ce - Yb)_N = 1.85$ to $4.47\}$. The samples from Tegar village and Sati bridge are moderately enriched in REE. Volcanics of Tegar village show REE enrichment from 101 -141 x chondrite for Light Rare Earth Elements (LREE) and 9 -14 x chondrite for Heavy Rare Earth Elements (HREE) with low to moderate negative Eu anomaly (Eu/Eu*= 0.46 - 1.02) (Text-figure 9). The chondrite normalized REE pattern of Sati bridge volcanics (Text-figure 10) suggest that the LREE are comparatively less enriched with ratio $\{(La/Sm)_N = 1.7 - 4.3\}$ whereas in Shukur the ratio is very low $\{(La/Sm)_N = 1.4 - 3.2\}$. The HREE contents are almost uniform for all the samples $\{(Gd/Yb)_N = 0.99 - 2.5\}$. The chondrite normalized REE pattern (Text-figure 8) for Shukur volcanics indicate that these rocks may belong to a primitive N - MORB to E - MORB. The Tegar village and Sati bridge volcanics, however, resembles to transitional nature of the basalts between E - MORB to OIB (Text-figures 9, 10). No radiometric data are available from the Shyok Volcanics.

Tirit Granitoids

Several granitic plutons are exposed immediately in the south of the Shyok Suture (Text-figures 2, 3, 4, Plate 1a). We call these WNW-ESE aligned plutons collectively the Tirit Granitoids. They consist of mildly deformed medium-to coarse-grained rocks, subleucocratic to mesocratic, relatively rich in ferromagnesian minerals and compositionally ranging from granodiorite-tonalite to gabbrodiorite. At several places they were intruded by vertical, undeformed, NW-SE trending

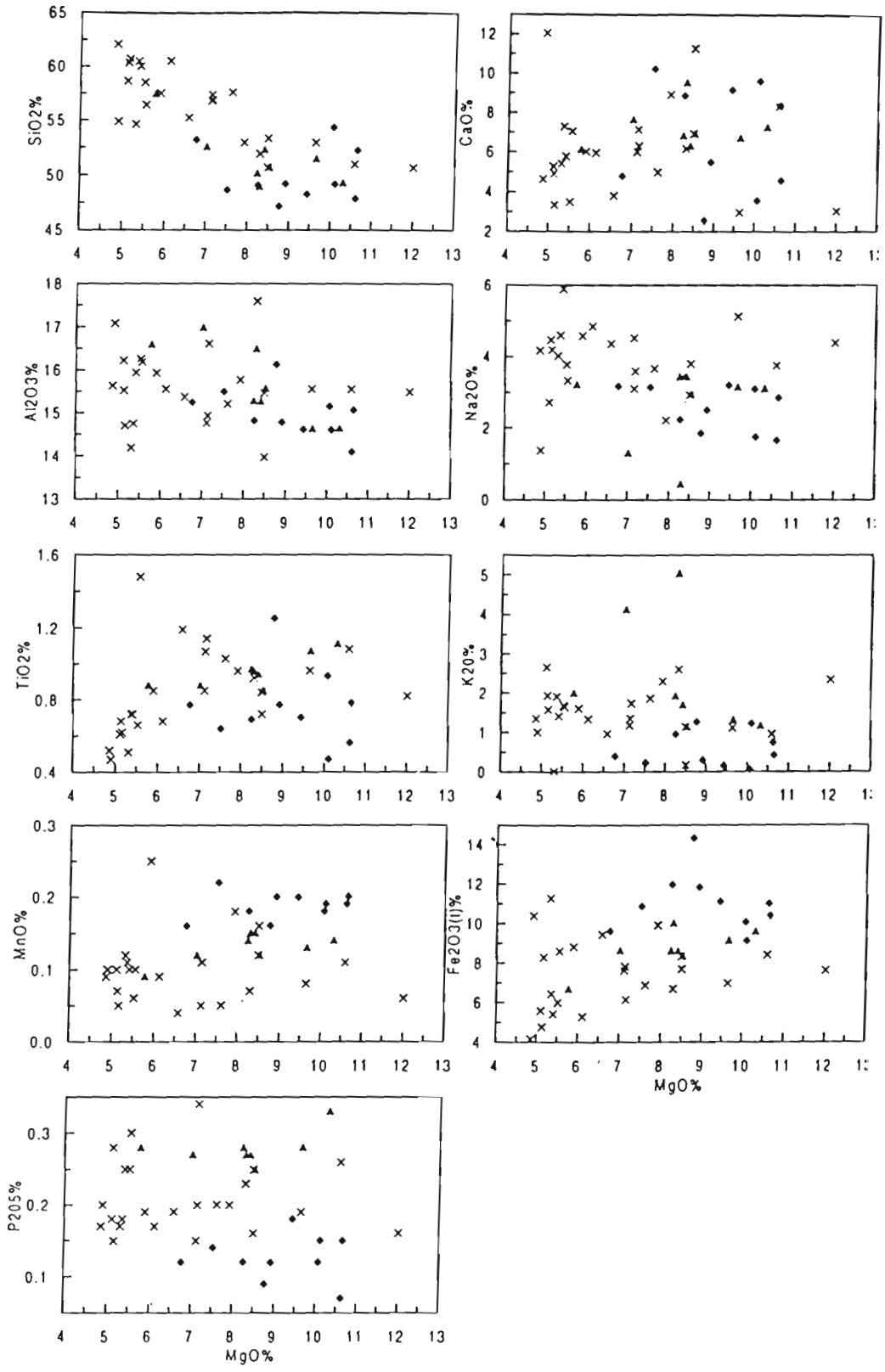

Text-figure 6–Major oxides versus MgO% variation diagrams for Shyok Volcanics. Symbols as in Text-figure 5.

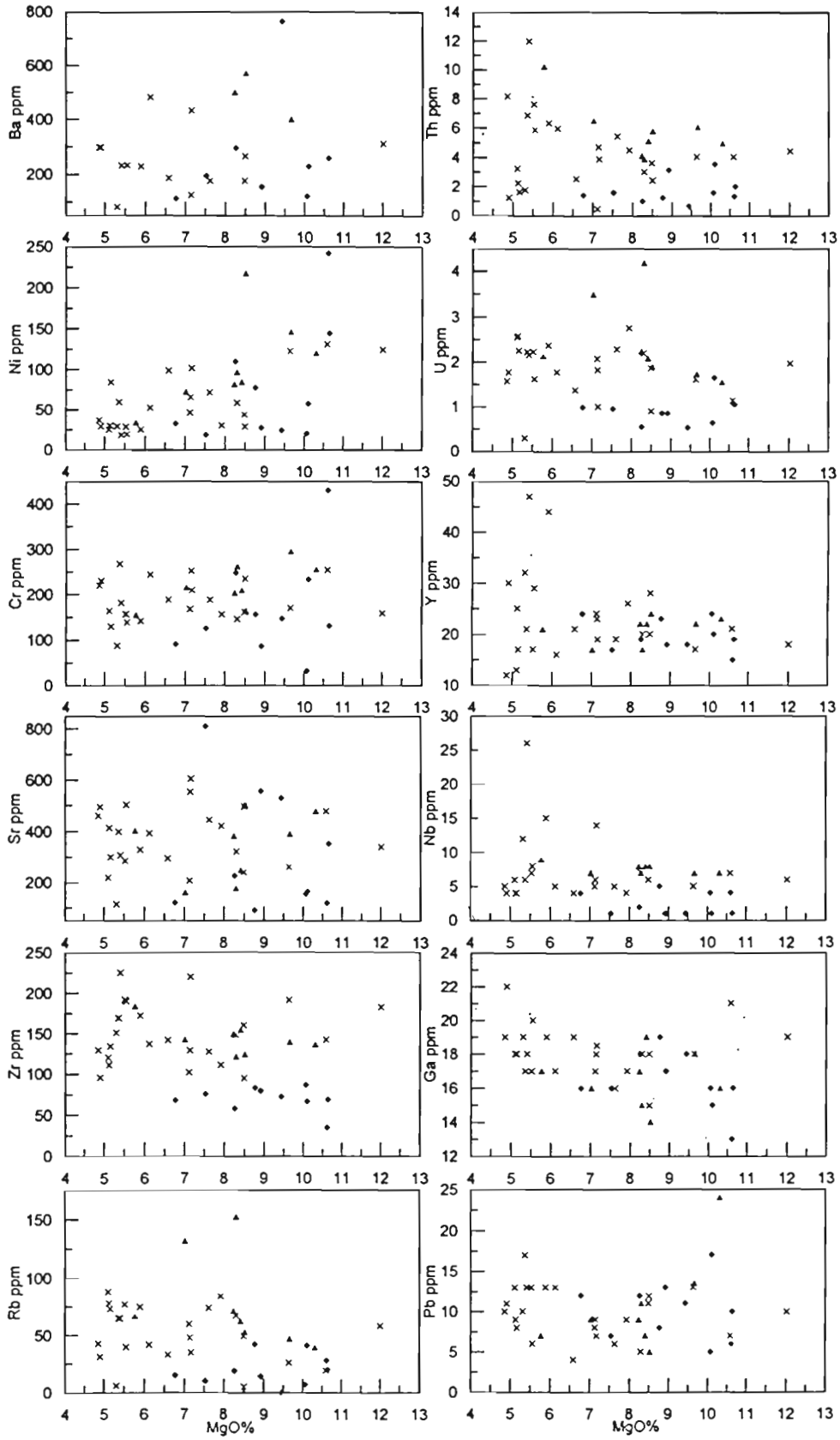

Text-figure 7–Trace element versus MgO% variation diagrams for Shyok Volcanics. Symbols as Text-figure 5.

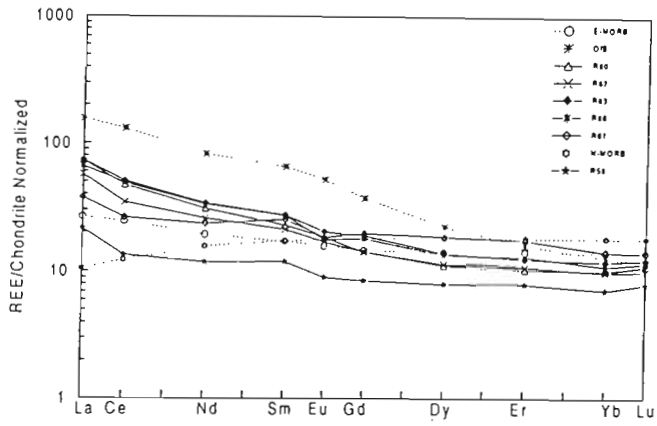

Text-figure 8–Chondrite normalised REE pattern for Shukur volcanics (normalising values and data for N-MORB, E-MORB and OIB after Sun & Mc Donough, 1989).

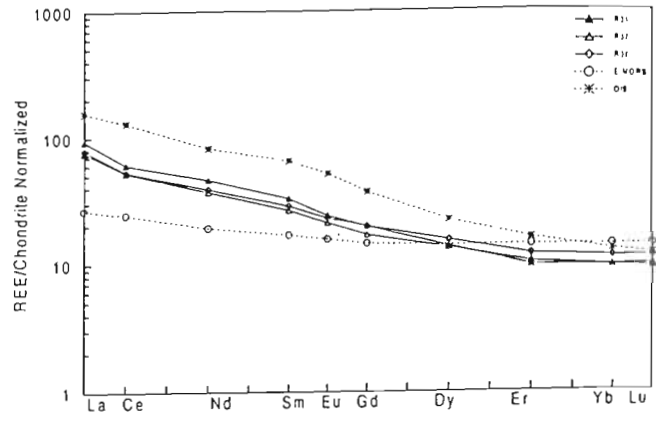

Text-figure 10–Chondrite normalised REE pattern for Sati bridge volcanics (normalising values and data for N-MORB, E-MORB and OIB after Sun & Mc Donough, 1989).

basic dykes that are 0.5-1 m thick. The granitoids are more basic at their margins than in the core and show hybridization and chilled margins along the intrusive contacts with the Shyok Volcanics. Fine-to medium-grained mafic xenoliths with sharp boundaries are common and range from a few mm to 50 cm in diameter. At some places metasedimentary enclaves are also present.

The Tirit Granitoids consist of plagioclase (oligoclase-andesine), K-feldspar, quartz and mafic minerals. Plagioclase laths are euhedral and enclosed within subhedral grains of K-feldspar and quartz. Most plagioclase crystals contain secondary sericite and epidote. Hornblende is abundant in diorites. The granodiorites display graphic intergrowth between quartz and feldspar, and plagioclase laths exhibit oscillatory zoning. Biotite is partly altered to green chlorite. The tonalites have lower K-feldspar and quartz contents than the granodiorites. Zircon, apatite, opaques and epidote are common accessory minerals.

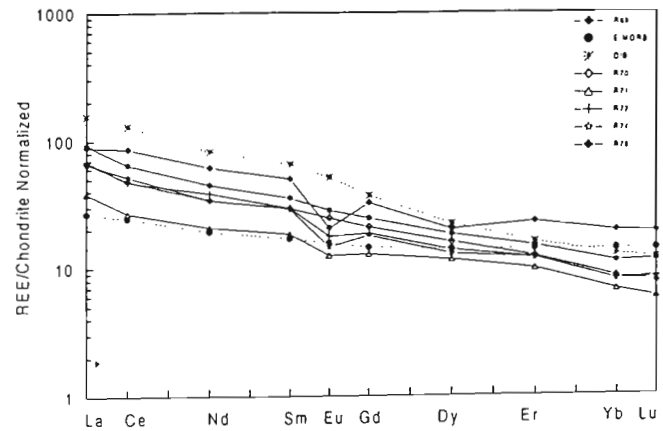

Text-figure 9–Chondrite normalised REE pattern for Tegar volcanics (normalising values and data for N-MORB, E-MORB and OIB after Sun & Mc Donough, 1989).

Geochemistry of the Tirit Granitoids

A total of 31 samples of Tirit Granitoids were analyzed and 10 representative examples are presented in Table 2. The analytical procedures are the same as for the Shyok Volcanics.

The Tirit Granitoids have a wide range of SiO_2 content (56.39 to 70.83 wt% , Table 2). The rocks thus range from quartz-diorite to tonalite, granodiorite and granitic rocks (Text-figure 11). The Al_2O_3 and CaO contents are generally high (15.3 to 17.08 wt% and 2.48 to 7.07 wt%, respectively). The high concentration of Al_2O_3 and CaO may be related to the plagioclase composition that remains relatively calcic even in silica-rich rocks. In most samples the relative concentration of Na_2O exceeds that of K_2O. According to AFM (Na_2O+K_2O-FeO*-MgO) and QBF diagrams (Text-figures 12, 13) where Q = {Si/3-(K+Na+2Ca/3)}, B = (Fe+Mg+Ti) and F = {555-(Q+B)} the Tirit Granitoids reflect at least for their major part a subalkaline trend intermediate between calcalkaline and alkaline.

Major element Harker variation diagrams (Text-figure 14) show a marked decrease in MgO with increasing SiO_2. Similar trends are shown by Fe_2O_3 and TiO_2. Though a general decrease is shown by Al_2O_3, CaO and P_2O_5, the trends are not well defined. Both major alkali oxides (Na_2O and K_2O) increase with increasing values of SiO_2, but the data points are more scattered. The co-linear, smooth and coherent variation trends of most major oxides suggest magmatic differentiation. In general, no compositional gap seems to exist among the Tirit Granitoids. All rocks of this suite appear to be co-magmatic.

A wide variation of trace elements has been measured (Table 2, Text-figure 15) particularly in Ba (163 to 629 ppm), Rb (5 to 158 ppm), Sr (237 to 507 ppm) and Zr (117 to 338 ppm) but also in Ni (3 to 33.2 ppm), Pb (1 to 28 ppm) and Cu (1 to 57.3 ppm). The granitoids are depleted in Nb (5 to 14

Table 2—Representative geochemical composition of Tirit granitoids.

Rock Type	mzdq, IV	dq, IV	mzdq, IV	gd, IV	ad, IV	mzdq, IV	gd, IV	gd, IV	gd, IV	gd, IV
S. No.	R57	R2	R6	R9	R3	R16	R28	R12	R24	R19
Major Oxides (wt%)										
SiO_2	56.39	57.16	65.62	66.18	66.59	67.72	68.3	69.04	69.09	70.19
TiO_2	1.1	0.68	0.53	0.53	0.53	0.48	0.47	0.4	0.44	0.39
Al_2O_3	16.11	15.88	16.54	16.25	15.96	16.15	16.1	16.13	15.98	15.5
Fe_2O_3(t)	8.25	7.27	3.93	4.03	3.9	3.59	2.67	2.61	2.6	2.81
MnO	0.12	0.13	0.04	0.04	0.04	0.05	0.04	0.02	0.03	0.05
MgO	5.85	5.24	1.59	1.52	1.47	1.23	1.12	1.06	1.05	0.83
CaO	7.03	7.01	2.97	3.28	2.95	3.33	3.65	2.98	3.52	2.48
Na_2O	3.05	3.7	4.36	4.31	4.04	4.34	4.62	5	4.84	4.17
K_2O	2.63	2.13	4.07	3.62	4.11	3.71	3.37	3.61	3.42	3.99
P_2O_5	0.31	0.24	0.19	0.21	0.19	0.23	0.21	0.19	0.21	0.17
LOI	0.57	0.64	0.93	0.62	0.86	0.81	0.47	0.41	0.43	0.52
Total	101.41	100.08	100.77	100.59	100.64	101.64	101.02	101.45	101.61	101.1
Trace Elements (ppm)										
Ba	342	358	468	441	524	551	467	570	513	572
Ni	18.5	n.d	31	33	33	25	15	19	15	18
Cu	57.3	n.d	10	27	22	8	6	7	5	6
Zn	77.9	n.d	0	0	1	2	b.d	b.d	b.d	6
Ga	16	n.d	17	17	15	16	19	17	15	15
Pb	4	n.d	15.2	11.5	19.5	5.3	8.7	14.5	9	13.4
Th	1.6	n.d	26	30	28	21	17	20	16	19
Rb	117	n.d	158	146	149	125	81	96	76	127
U	0.9	n.d	8.4	7.3	7.8	6.1	3.1	4.3	2.7	6.7
Sr	315	n.d	289	294	263	282	309	311	299	237
Y	20	n.d	34	31	31	31	31	27	30	24
Zr	117	n.d	239	219	237	206	211	182	200	173
Nb	6	n.d	8	7	7	6	5	7	6	5
Rare Earth Elements (ppm)										
La	n.d	29.3	36.8	34.2	43.6	23	23.8	17.6	21.9	21.5
Ce	n.d	37.2	57.1	52.6	64.4	35.1	42	29.8	38	32.8
Nd	n.d	15.7	24.1	20.5	25	15.8	19.3	13.3	17.1	14.1
Sm	n.d	3.82	5.07	4.65	5.14	4.04	4.87	3.25	4.36	3.3
Eu	n.d	1.15	1.08	0.88	0.99	0.9	1.06	0.76	1	0.78
Gd	n.d	3.09	3.68	3.5	3.7	3.23	3.11	2.47	2.74	2.43
Dy	n.d	2.63	3.5	3.2	3.34	3.17	3.44	2.42	3.12	2.36
Er	n.d	1.61	1.96	1.85	1.93	1.74	1.99	1.4	1.79	1.37
Yb	n.d	1.73	2	1.87	1.75	1.7	2.2	1.47	1.9	1.4
Lu	n.d	0.246	0.281	0.259	0.259	0.237	0.283	0.197	0.25	0.2
CIPW Norm										
q	4.94	5.23	15.09	17.24	19.09	18.97	19.5	18.4	19.4	23.58
or	15.54	12.59	24.05	21.39	24.29	21.93	19.92	21.33	20.21	23.58
ab	25.81	31.13	36.89	36.47	34.19	36.72	39.09	42.31	40.96	35.29
an	22.5	20.43	13.49	14.3	13.28	13.63	13.24	10.91	11.78	11.19
di	8.36	10.33	-	0.49	0.09	1.15	2.86	2.16	3.53	0.22
C	-	-	0.02	-	-	-	-	-	-	-
hy	17.06	14.33	7.02	6.7	4.31	5.32	3.33	3.52	2.78	4.28
mt	3.22	2.84	1.54	1.57	5.65	1.39	1.04	1.01	1.01	1.09
il	2.09	1.29	1.01	1.01	1.01	0.91	0.89	0.76	0.84	0.74
ap	0.72	0.56	0.44	0.49	0.44	0.53	0.49	0.44	0.49	0.39
Plagioclase	An47	An39	An27	An28	An28	An27	An25	An20	An22	An24
A/CNK	0.67	0.74	0.97	0.96	0.97	0.94	0.9	0.92	0.88	0.99

n.d. = not determined

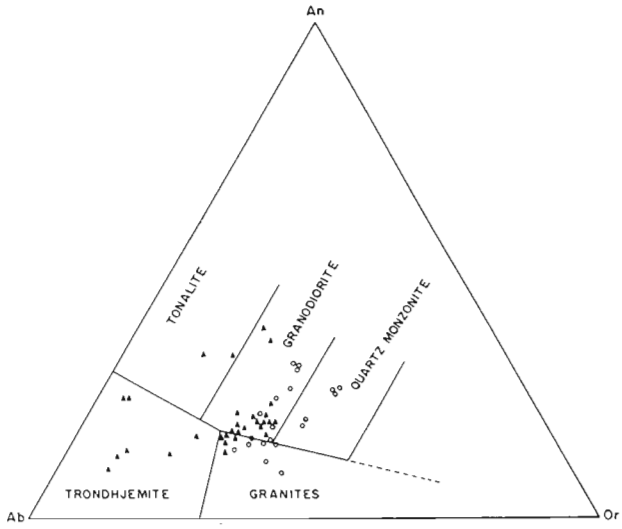

Text-figure 11–An-Ab-Or classification diagram for the Tirit and Karakoram Granitoids (plotted on the diagram after 'O' Connor (1965). Dark triangles = Tirit Granitoids; open circles=Karakoram granitoids.

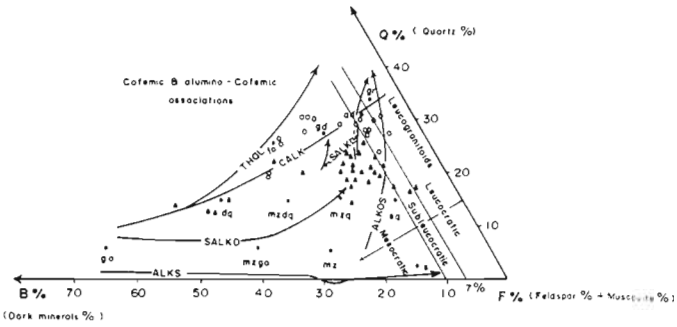

Text-figure 13–Q-B-F diagram shows the subalkaline to calcalkaline trend with cafemic association for Tirit Granitoids, and cafemic and alumino-cafemic associations for Karakoram Granitoids (plotted on the diagram after Debon & Le Fort 1983, 1988). Dark triangles = Tirit Granitoids; open circle = Karakoram granitoids. Different rock types presented in the diagram are: **gr**=granite, **ad**=adamellite, **gd**=granodiorite, **to**=tonalite, **sq**=quartz syenite, **mzq**=quartz monzonite, **mzdq**=quartz monzodiorite, **dq**=quartz diorite, **s**=syenite, **mz**=monzonite, **mzgo**=monzogabbro, **go**=gabbro.

ppm) which suggests arc magmatism. All the samples are rich in Sr (237 to 507 ppm); the tonalite samples have very low contents of Rb (5 to 59 ppm) and very high Sr contents (314 to 507 ppm). This may reflect the higher plagioclase percentage in these rocks. The Rb/Sr value for Tirit Granitoids is low (<1). Similarly, the molar A/CNK value (Aluminous Saturation Index (ASI) of Zen (1986); where molar A/CNK = Al_2O_3/Na_2O+K_2O+CaO ratio) in the Tirit Granitoids ranges between 0.67 to 1.04 (Table 2) and suggests a metaluminous nature of these intrusions. A similar relationship can also be evidenced from a A/CNK versus SiO_2% diagram (Text-figure 16) and also by high normative diopside and corundum values (Table 2). Furthermore, if we follow the classification scheme of Chappel and White (1974) and plot our data, it could be

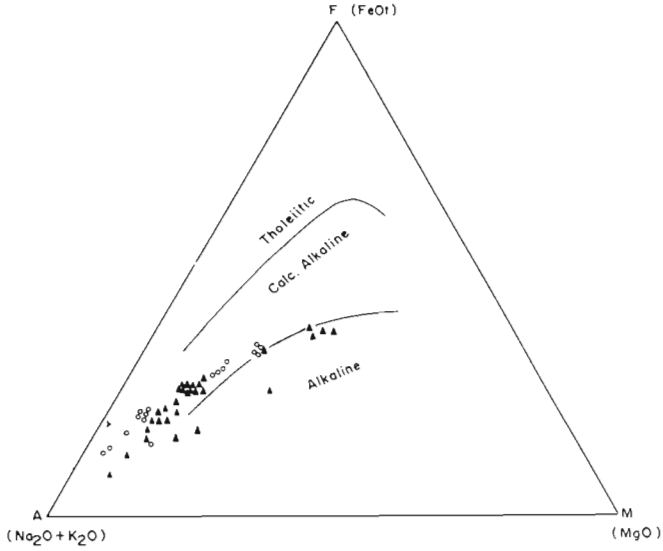

Text-figure 12–AFM diagram for the Tirit and Karakoram granitoids. Dark triangles=Tirit Granitoids; open circles = Karakoram granitoids.

suggested that the Tirit Granitoids are I-type (Text-figure 16). The Y/Nb ratio is > 2 what further suggests island arc magmatism. The trace elements versus SiO_2 variation diagrams for the Tirit Granitoids (Text-figure 15) mostly show that the concentrations of Rb, Y, Zr, Zn, Nb, U and Ga are systematically decreasing with increasing contents of silica. The scattering of some trace elements (Ba, Sr, Th) may be due to a heterogeneous accumulation of some essential and accessory mineral constituents which are rich in these elements (Pearce & Norry, 1979).

The chondrite normalised (Sun & Mc Donough, 1989) REE patterns (Text-figures 17 a, b) are similar for most samples. According to Holtz (1989) the REE concentration in a batholith is strongly enriched in Light Rare Earth Elements (LREE) (La = 20-100 x Chondrite) and depleted in Heavy Rare Earth Elements (HREE) (Yb = 0.5-8 x Chondrite). In the case of the Tirit Granitoids these values are: La = 17-43.6 x chondrite, and Yb = 1.4 -2.37 x chondrite which is consistent with the values of granitoids. All the samples are moderately fractionated in their REE contents {$(La/Lu)_N$ = (8.05-18.1)}. Over all the REE patterns show an enrichment and a good fractionation in LREE {$(La/Sm)_N$ = 2.92 to 5.47} than HREE {$(Gd/Lu)_N$ = (1.35-1.78)} with marked negative Eu anomalies, which indicates feldspar fractionation. The Eu/Eu* values range from 0.66 to 1.02. The chondrite normalised REE patterns further show a flat MREE (Middle Rare Earth Element)-HREE pattern with Gd = 2.43-4.44 x chondrite and Yb = 1.4-2.37 x chondrite. Such a MREE-HREE flat pattern is due to the presence of garnet in the residue melt (Henderson, 1984). The depletion in HREE contents is mainly controlled by the fractionation of garnet from the source melt. The primitive mantle (Sun & Mc Donough, 1989) normalized trace-element patterns (Text-figure 18) show a systematic depletion in Ti, P, Sr, Nb and Ba. This depletion is typical of the calcalkaline magmatism of a subduction zone environment. The Nb versus Y, and Rb versus Y+Nb plots (Text-figure 19)

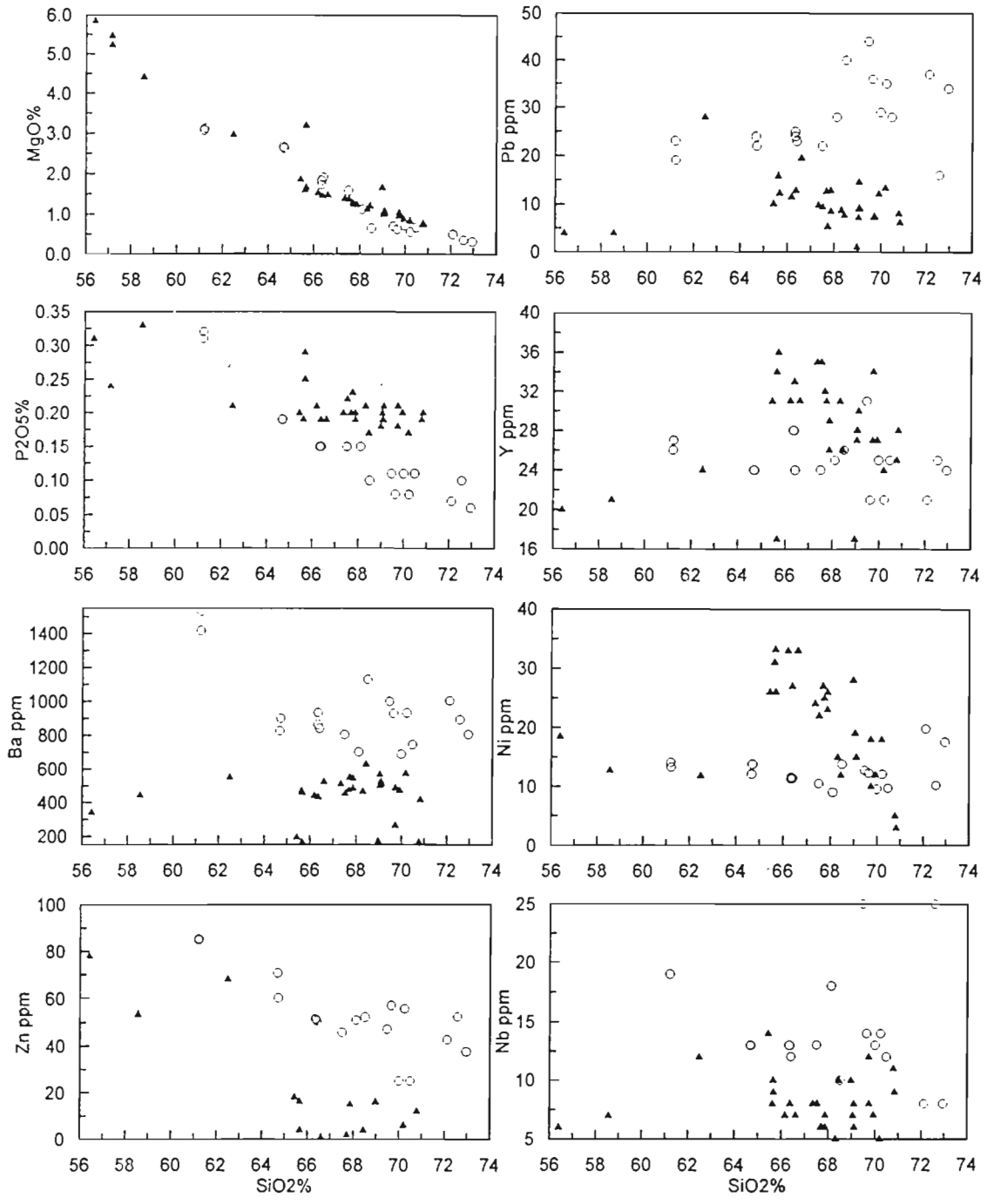

Text-figure 14–Harker variation diagrams for major oxides. Dark triangles = Tirit Granitoids; open circles = Karakoram granitoids.

further confirm the volcanic arc origin of the Tirit Granitoids.

According to Pearce *et al.* (1984) this type of granitoid may be designated as a post-collision granitoid which is formed by melting of the lower crust as a result of thermal relaxation followed by collision and/or also from the melting of the upper mantle due to adiabatic decompression which accompanies post-collision uplift and erosion.

Karakoram Batholith

The Karakoram Batholith, which lies immediately in the north of the Shyok Suture Melange is one of the most important terrane in the eastern Karakoram, which alongwith its metamorphic assemblages represent the southern margin of Asia (Sinha *et al.*, 1999) (Text-figures 2, 3, 4, Plate 1c). The batholith and its associated metamorphic rocks constitutes the

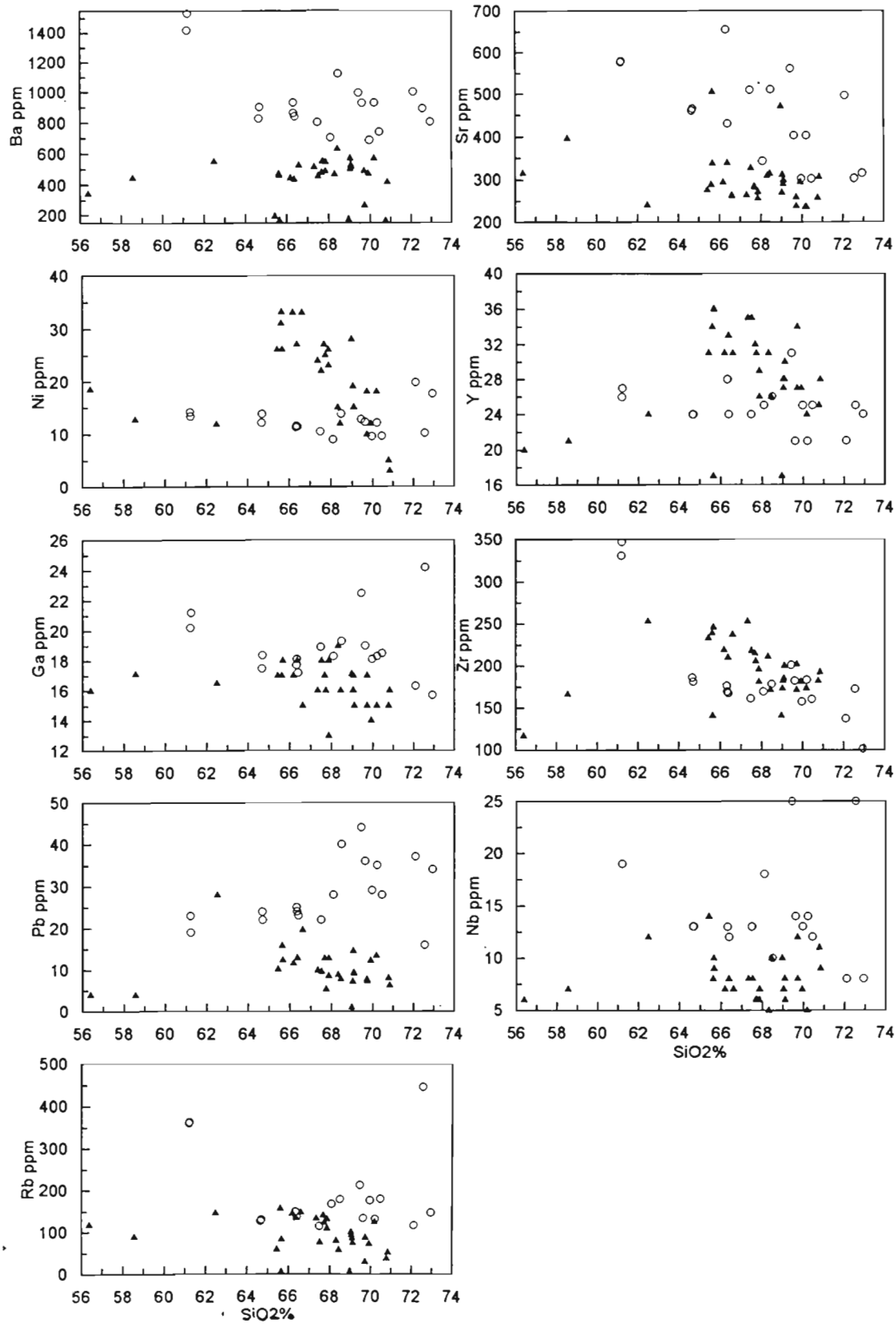

Text-figure 15–Harker variation diagrams for trace elements. Dark triangles = Tirit Granitoids: open circles = Karakoram Granitoids.

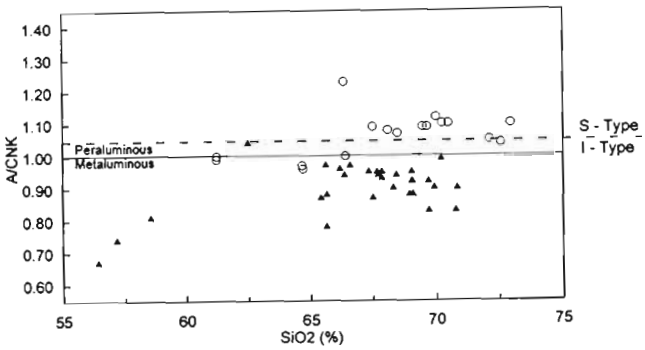

Text-figure 16–SiO_2 versus A/CNK diagram for Tirit and Karakoram Granitoids showing metaluminous, I-type and peraluminous, S-type granitoids respectively (plotted on the diagram after White & Chappell 1977). Dark triangles = Tirit Granitoids; open circles = Karakoram granitoids.

southern part of the eastern Karakoram. The southern contact of the batholith is partly intrusive into, partly faulted against the Shyok Suture Melange (Text-figures 2, 3, 4). The batholith represents a morphologically elevated terrain in the north of the Nubra-Shyok valleys, extending almost parallel to the Shyok Suture (Text-figures 2, 4, Plate 1c). At several places, the sharp contact between the Shyok Suture and Karakoram Batholith is defined by the NW-SE trending Karakoram strike-slip fault zone, which is punctuated by hot springs. The southern boundary of the Karakoram Batholith is defined by mylonites and a ~ 50 m wide zone of metamorphic rocks. The metamorphic rocks are strongly foliated carbonaceous slates, marbles, metaconglomerates, quartzites, micaschist and gneisses.

Near the Shyok Suture Melange the Karakoram Granitoids are leucocratic, coarse-grained, porphyritic orthogneiss. The gneissic character of these rocks decreases northward and the rocks gradually pass into porphyritic granites and granodiorites. The most common rocks of the Karakoram Batholith are weakly to moderately deformed muscovite- and biotite-bearing two mica granites, hornblende-biotite granitoids and medium- to coarse-grained K-feldspar rich granites, enclosing large xenoliths of metasedimentary and mafic rocks. Compositionally, the Karakoram Batholith ranging from granite to quartz monzonite, granodiorite, and tonalite (Text-figure. 11). Aplites, pegmatite dykes, fine grained quartz-feldspathic veins and dykes of intermediate composition are common. The granitic batholith intruded the Carboniferous-Permian sequence of the Karakoram Tethyan zone to the north (Sinha *et al.*, 1999).

Geochemistry of the Karakoram Batholith

Eighteen representative samples of Karakoram Granitoids were analysed for major, trace and rare earth elements (REE); nine representative analyses are given in Table 3. The analytical procedures are the same as for the Shyok Volcanics.

The Karakoram Granitoids have a range of SiO_2-content from 61.2 to 72.95 wt%. This composition ranges from quartz monzonite to granodiorite and granite, they further show a wide range in Al_2O_3 (14.77 to 16.67 wt%) and CaO (1.14 to 4.32 wt%). Granitoids with lower silica contents (61.22 to 64.7 wt%) have higher values of Al_2O_3 (16.53 wt%), CaO (3.85

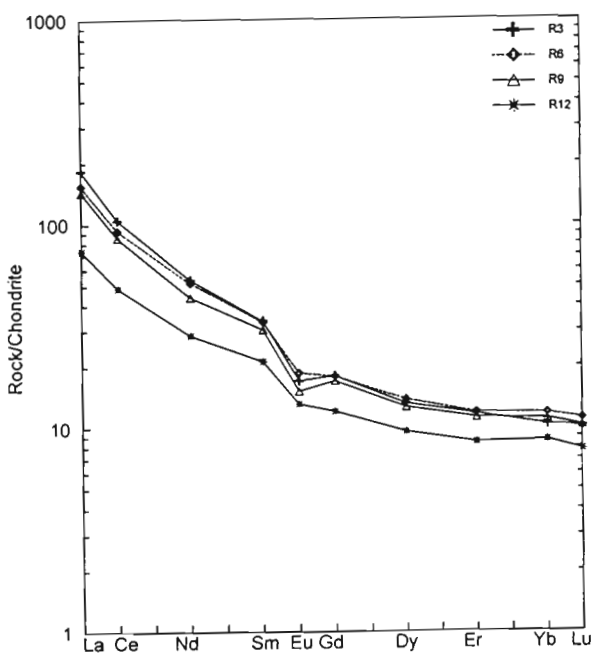

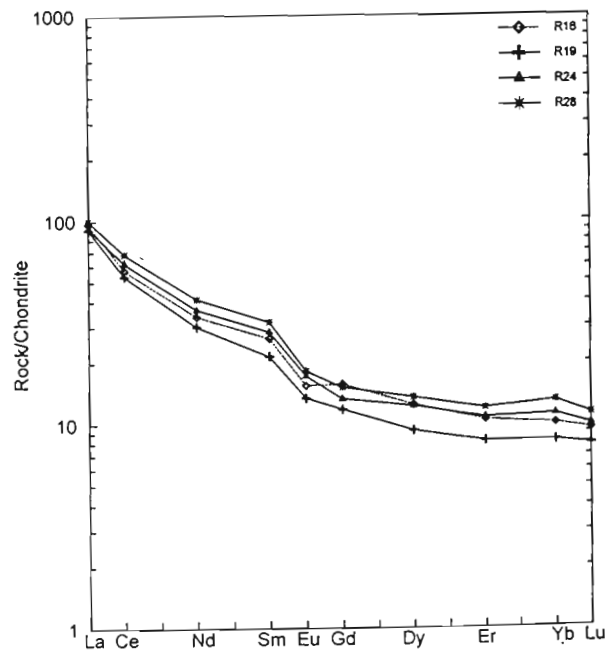

Text-figure 17a, b.–Chondrite-normalised REE plots for Tirit Granitoids (normalising values after Sun & Mc Donough 1989).

Table 3—Representative geochemical composition of Karakoram granitoids.

Rock Type	mzq, IV	ad, III	gd, III	gd, IV	gd, II	gd, II	ad, II	ad, I	ad, I
S.No.	K20	K18	K14	K11	K9	K6	K17	K13	K4
Major Oxides (wt%)									
SiO_2	61.22	66.33	66.4	67.49	68.1	68.49	69.93	72.11	72.57
TiO_2	0.76	0.5	0.5	0.45	0.45	0.33	0.29	0.23	0.2
Al_2O_3	16.67	15.96	15.41	15.47	15.46	16.46	15.63	15.13	14.77
Fe_2O_3(t)	6.11	3.89	4.3	3.6	3.22	2.36	2.35	1.87	1.51
MnO	0.09	0.08	0.08	0.06	0.05	0.03	0.04	0.03	0.04
MgO	3.12	1.82	1.9	1.57	1.11	0.64	0.62	0.49	0.35
CaO	3.87	2.29	3.5	3.04	2.53	2.17	2.02	1.91	1.14
Na_2O	2.76	2.9	3.14	3.2	3.56	4.3	4.3	4.47	4.28
K_2O	4.74	3.75	3.56	3.2	3.56	3.99	3.52	3.3	4.74
P_2O_5	0.32	0.15	0.15	0.15	0.15	0.1	0.08	0.07	0.1
LOI	0.62	2	1.8	1.7	1.04	0.7	0.8	0.8	0.7
Total	100.37	99.67	100.74	99.93	99.23	99.57	99.58	100.41	100.26
Trace Elements (ppm)									
Ba	1531	933	841	804	702	1129	927	1004	893
Ni	13.3	11.3	11.4	10.5	9	13.8	12.3	19.8	10.2
Cu	14.7	10.1	10.9	7.9	8.9	5.5	5.8	4.9	5.1
Zn	85.3	51.4	50.6	45.7	50.9	52.1	57	42.6	52.3
Ga	21.2	17.7	17.2	18.9	18.3	19.3	19	16.3	24.2
Pb	19	25	23	22	28	40	36	37	11.6
Th	16.3	23.9	15.2	11.8	13.4	25.9	24.8	27.2	11.8
Rb	364	150	139	116	170	181	136	119	447
U	3.1	5.3	4.3	2.2	4	3.7	3.3	3.8	6.1
Sr	579	654	430	509	343	511	402	496	303
Y	27	28	24	24	25	26	21	21	25
Zr	347	176	167	161	169	178	182	137	172
Nb	19	13	12	13	18	10	14	8	25
Rare Earth Elements (ppm)									
La	113.1	62.2	42.4	36.5	39.35	41.9	31.1	33.3	52.2
Ce	221.2	125.3	78.9	62.9	69.3	76.3	60.8	63.3	96.2
Nd	72.8	38.9	28.1	25.7	27.6	28.8	21.2	22.7	35.3
Sm	12.2	6.99	5.54	5.98	6.24	5.86	3.11	4.2	6.53
Eu	2.08	1.17	1.07	1.204	0.995	0.964	0.505	0.963	0.904
Gd	7.6	4.81	4.27	3.89	4.11	3.45	2.08	2.73	3.4
Dy	4.18	3.39	3.4	3.06	3.14	1.97	0.94	1.59	1.82
Er	1.46	1.37	2.08	1.7	1.62	0.93	b.d	0.71	0.9
Yb	1.51	1.62	1.76	1.49	1.32	0.58	0.243	0.56	0.685
Lu	0.213	0.255	0.351	0.225	0.175	0.133	0.019	0.239	0.104
CIPW Norm									
q	12.74	26.48	22.99	26.88	25.95	22.04	25.25	28.16	26.29
or	28.01	22.16	21.04	18.91	21.04	23.58	20.8	19.5	28.01
ab	23.35	24.54	26.57	27.08	30.12	36.39	36.39	37.82	36.22
an	17.11	10.38	16.38	14.1	11.57	10.11	9.5	9.02	5
di	0.73	3.33	0.39	1.57	1.51	1.36	1.57	0.9	0.77
C	-	-	-	-	-	-	-	-	-
hy	12.69	7.67	8.27	6.81	5.33	3.46	3.45	2.74	2.11
mt	2.38	1.52	1.68	1.41	1.16	0.87	0.92	0.72	0.58
il	1.44	0.95	0.95	0.85	0.85	0.63	0.55	0.44	0.38
ap	0.74	0.35	0.35	0.35	0.35	0.23	0.19	0.16	0.23
Plagioclase	An42	An30	An38	An34	An28	An22	An21	An19	An12
A/CNK	1	1.23	1	1.09	1.08	1.07	1.09	1.05	1.04

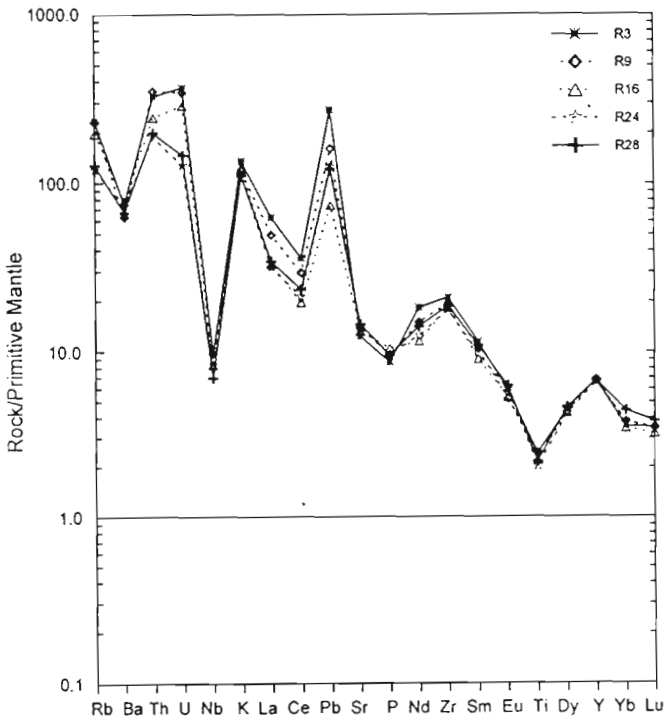

Text-figure 18–Primitive mantle normalised trace element plots for the Tirit Granitoids (normalised values after Sun & Mc Donough 1989).

wt%), TiO_2 (0.75 wt%), Fe_2O_3(t) (6.1 wt%) and P_2O_5 (0.32 wt%) which suggests a quartz-monzonite composition. Except for the quartz monzonite, most of the major oxide versus SiO_2 plots show a systematic decrease in major oxides with increasing values of silica (Table 3; Text-figure 14). According to the AFM and QBF diagrams (Text-figures 12, 13) the Karakoram Granitoids are following both calcalkaline and subalkaline trends. The Karakoram Granitoids have higher A/CNK values which ranges between 0.96 to 1.23 and suggests both a metaluminous and peraluminous nature (Table 3). According to SiO_2 versus A/CNK diagram (Text-figure 16) the Karakoram Granitoids are both I- and S-types. Trace elements versus SiO_2 variation diagrams (Text-figure 15) show that Rb, Y, Zr, Sr and Nb elements systematically decrease with increasing values of silica; Pb shows a good negative correlation. Chondrite normalised REE patterns (Text-figures 20 a, b) suggest that all samples are strongly enriched in Light Rare Earth Elements (LREE) (La=31.1-113.1 x Chondrite) and depleted in Heavy Rare Earth Elements (HREE) (Yb=0.56-1.76 x Chondrite). This indicates that the Karakoram Granitoids are more LREE enriched than the Tirit Granitoids. All the samples are highly fractionated in their total REE contents with a $(La/Lu)_N$ ratio of 12.95 to 56.94. An enrichment in LREE is also observed in the ratio $(La/Sm)_N$=3.94 to 5.98 and a depletion in HREE in the ratio $(Gd/Lu)_N$=1.41 to 4.41. The primitive mantle normalised trace-element patterns (Text-figure 21) show a systematic depletion in Ti, P, Sr, Nb and Ba. This depletion is typical of a calcalkaline magmatism in a subduction zone environment. Similarly the Nb versus Y, and Rb

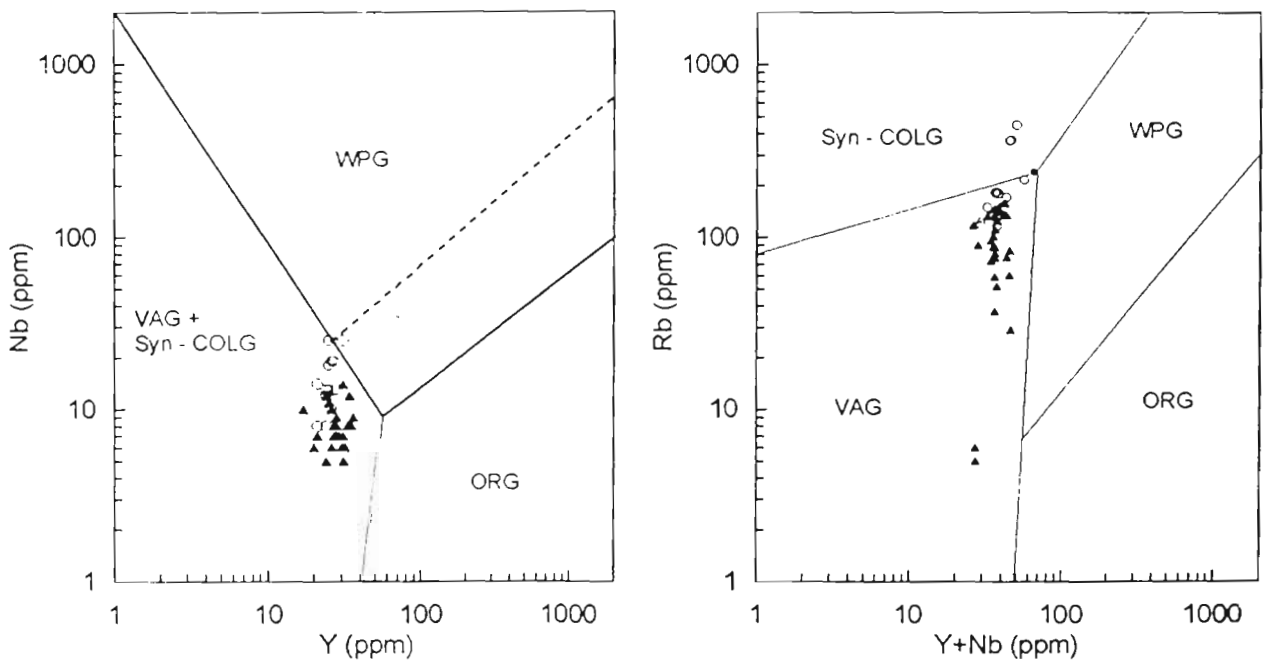

Text-figure 19–Nb-Y and Rb-Y+Nb tectonic discrimination diagrams showing volcanic arc granite (VAG) + syn-collision granite (Syn-COLG) setting for the Tirit and Karakoram Granitoids respectively (plotted on the diagram after, Pearce *et al.*, 1984). Dark triangles = Tirit Granitoids; open circle = Karakoram Granitoids.

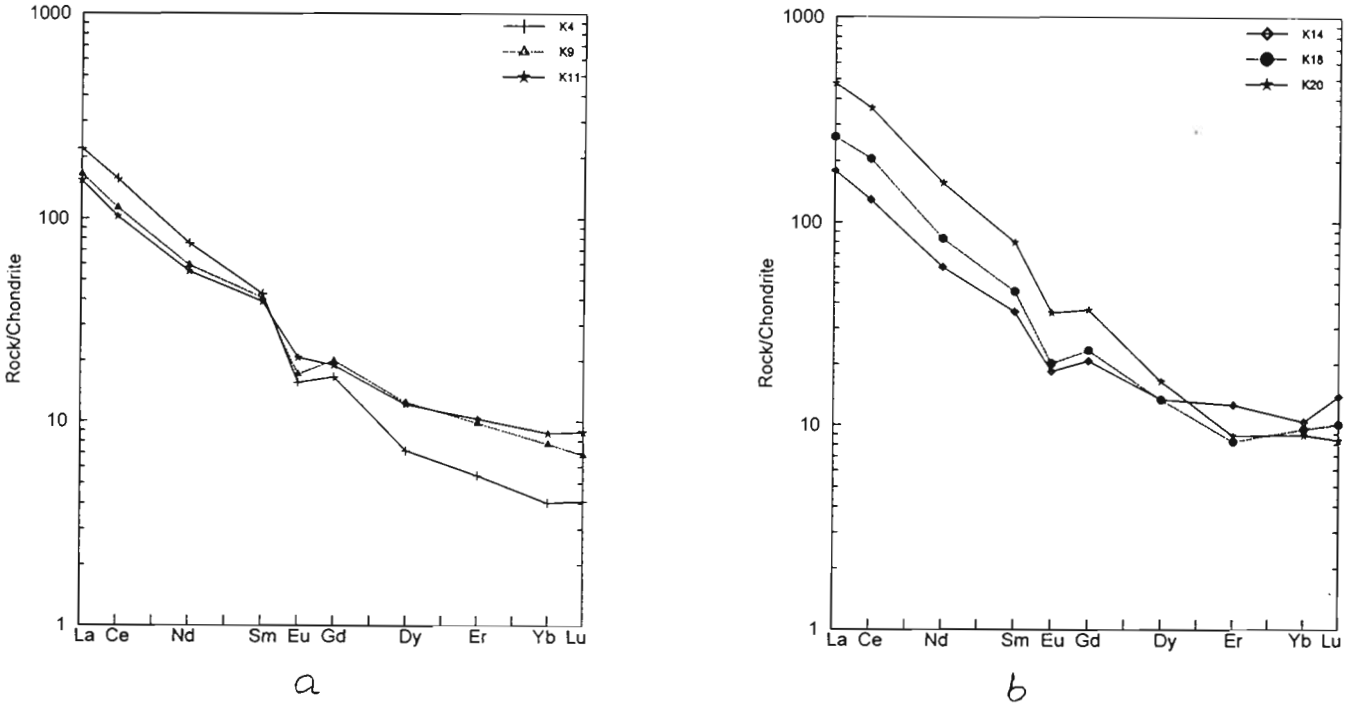

Text-figure 20 a, b–Chondrite-normalised REE plots for the Karakoram Granitoids (normalised values after Sun & Mc Donough 1989).

versus Y+Nb diagrams (Text-figure 19) suggest that the Karakoram Granitoids display chemical characters of both the VAG (volcanic arc granite) and the Syn-COLG (syn-collision granite).

The volcanic arc granitoids of the Karakoram also show a close compositional affinity with the continental arc plutonism recorded from the Chile arc (Baldwin & Pearce, 1982), which is further supported by the occurrence of both the I- and S-type granitoid signatures and the depletion in Ti, P, Sr, Nb, and Ba (Text-figure 21). Similarly, samples K4 and K20 (Table 2) from the Karakoram Granitoids show a significant enrichment in Rb, Ba, Large Ion Lithophile Elements (LILE) and a strong depletion in High Field Strength Elements (HFSE), which suggests a chemical signature similar to those of syn-collision granitoids.

We have dated three samples of the S-type granite collected from the middle part of eastern Karakoram Batholith by using Rb/Sr isotopic whole rock technique. These samples document syn-collisional arc magmatic signatures (Rakesh Chandra, 1999). This S-type granite is 83 ± 9 Ma old with an initial $^{87}Sr/^{86}Sr$ ratio of 0.7994 ± 0.00023 (Sinha *et al.*, 1997) (Text-figure 22).

Tectonic implication and Discussion

In the Shyok Suture Zone the high-Mg tholeiitic basalt and calc-alkaline andesites of the Shyok Volcanics have a subduction zone chemical signature; the calcalkaline andesites are intruded by the Tirit Granitoids, whereas the high-Mg tholeiitic basalt are overlain by Albian-Aptian *Orbitolina*-bearing limestones and turbidites of the Saltoro Formation (Upadhyay *et al.*, 1999). REE data on Shyok Volcanics indicate that at Shukur village these rocks show chemical signatures intermediate between primitive N-MORB to E-MORB). The Tegar village and Sati bridge volcanics, however, resembles to transitional nature of basalt between E-MORB to OIB. Interestingly, if we look into the data from the Northern Suture in Kohistan (Petterson & Windley, 1985, 1991; Pudsey , 1986; Coward *et al.*, 1986; Treloar *et al.*, 1996; Khan *et al.*, 1998), it appears that the Chalt Volcanics and overlying Aptian-Albian sediments (limestone and turbidites) of the Yasin group have a close similarity with the Shyok Volcanics and the Saltoro Formation (Upadhyay *et al.*, 1999).

Petterson and Windley (1985) stated that the arc-batholith growth in Ladakh is characterised by the Dras volcanic arc on the south side of the Ladakh Batholith, whereas in Kohistan the Chalt island arc volcanics are on the north side of the batholith. However, our data show that the Shyok Volcanics are exposed on the north side of the Ladakh Batholith which further suggest a correlation between the Chalt volcanics and Shyok Volcanics.

The mildly deformed trondhjemite-tonalite-granodiorite-and granite of the Tirit Granitoids are composite plutons located south of the Shyok Suture Melange. They intrude the Shyok Volcanics and Shyok Suture Melange. These granitoids

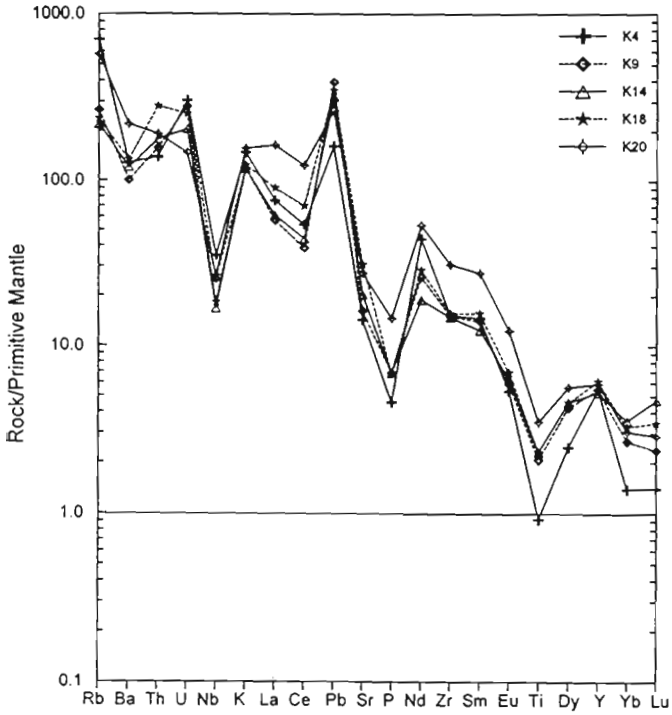

Text-figure 21–Primitive mantle normalised trace element plots for the Karakoram Granitoids (normalised values after Sun & Mc Donough 1989).

are subalkaline, I-type with volcanic arc chemical signatures. Incidently, the regional tectonic setting, the nature of occurrence and the composition of the Tirit Granitoids are very similar to the plutonic suites of northern Kohistan (Gindai, Matum Das and Nomal plutons of Petterson & Windley 1985, 1991; Debon *et al.* 1987). The northern Kohistan plutonic suites are also located immediately south of the Northern Suture Zone and intrude the Chalt Volcanics (Coward *et al.*, 1986), a tectonic situation similar to that of the Tirit Granitoids. This infers that similarity exist between the Tirit Granitoids and the plutonic suites of northern Kohistan. If this is true then the Tirit Granitoids should also yield ages similar to those reported by Petterson and Windley (1985) for the northern Kohistan plutons as 102 ± 12 Ma, 54 ± 4 Ma and 40 ± 6 Ma. No radiometric data are available on the Tirit Granitoids.

The eastern Karakoram Batholith is dominated by quartz monzonite-tonalite-granodiorite and granite. Unlike the Tirit Granitoids, the subalkaline to calcalkaline Karakoram Batholith is constituted by both I- and S- type granitoids with volcanic arc and syn-collision chemical signatures. Based on REE patterns the I-type granitoids document typical calcalkaline magmatism of a subduction zone environment. In contrast, most of the S-type granitoids are crust-derived, anatectic peraluminous granites.

Age data recorded from the Karakoram Batholith exposed along the Karakoram highway in northern Pakistan range mostly between the Jurassic & Early Cretaceous to Eocene and the Miocene (Brookfield and Reynolds, 1981; Reynold *et al.*, 1983; Le Fort *et al.*, 1983; Debon *et al.*, 1987; Zeitler, 1985). The occurrence of Eocene to Miocene ages from the Karakoram Batholith has been interpreted by some workers to indicate that the Northern Suture of Kohistan and the Shyok Suture of Ladakh are younger than the 50-60 Ma Indus Suture (Brookfield & Reynolds, 1981). However, based on Rb-Sr and $^{40}Ar/^{39}Ar$ data, Srimal *et al.* (1987) suggested an age range between 130 and 50 Ma for the eastern Karakoram batholith. According to them the composite Karakoram batholith represents at least two major sources for the magmas. The earlier Jurassic-Early Cretaceous phase represents a continental margin arc magmatism (I-type with $\delta\ ^{18}O$ values < + 8 ‰) and results from subduction along the North Saltoro (Shyok Suture) – Bangong-Nujiang Zone. The later Miocene S-type granites ($\delta\ ^{18}O$ value > + 9.5 ‰) are derived from crustal anatexis in the Miocene due to intracontinental thrusting along the rejuvenated North Saltoro Suture following the India-Asia collision. Recently, Ogasawara *et al.* (1994) dated hornblende and biotite from the Khunjerab pluton as 107 ± 5 Ma and 96.9 ±4.8 Ma respectively. A slightly younger K-Ar biotite ages of 84.2 ± 4.2 and 85.9 ± 4.3 Ma have been obtained by them for the north Sost pluton. Similarly, Debon and Khan (1996) obtained Rb-Sr age of 88±4 Ma ($^{87}Sr/^{86}Sr = 0.70440 \pm 7$) for the Karakoram Batholith located along the Karambar valley in northern Pakistan.

Recently acquired isotopic age data by us on three S-type granite samples of Karakoram batholith (Sinha *et al.*, 1997) indicates that this intrusive phase is 83 ± 9 Ma with an initial $^{87}Sr/^{86}Sr$ ratio of 0.7994 ± 0.00023 (Text-figure 22). This new age datum suggests a close similarity with the north

S. No.	Rb^{87}/Sr^{86}	Sr^{87}/Sr^{86}	Age
K4	5.21	0.7161	
K9	1.41	0.7115	83±9 Ma
K12	0.7	0.7108	

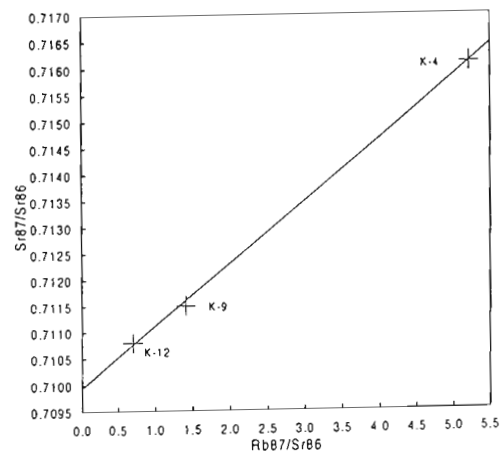

Text-figure 22–Rb-Sr whole rock isotopic data for Karakoram granitoid. $^{87}Rb/^{86}Rb$ versus $^{87}Sr/^{86}Sr$ isochron for three S-type Karakoram granitoid samples. Age = 83±9 Ma; initial ratio = 0.70994 ± 0.00023.

Sost pluton and Karambar valley pluton of main Karakoram Axial batholith exposed in northern Kohistan. The syn-collision nature (Rakesh Chandra, 1999) of these granitoids may indicate that the collision between Kohistan-Ladakh arc and Karakoram block was active 83 ± 9 Ma; which is in close agreement with the age of suturing of the Kohistan and Asia between 100 and 85 Ma (Petterson & Windley, 1991; Treloar *et al.*, 1996) . The above datum is also compatible with the fact that subduction-related magmatism may continue after initial collision for a period of as long as 30-50 Ma (Bonin, 1990). The above mentioned points further suggest that there are at least three stages of batholith growth in the eastern Karakoram region. The Jurassic-Early Cretaceous I-type granitoids most likely formed during subduction of the northern Ladakh margin beneath the Karakoram block followed by the collision-related S-type plutonism during 83 ± 9 Ma. The younger Miocene granitoids may perhaps indicate crustal anatexis along the Shyok Suture following the collision of Indian Plate along the Indus Suture during 50-60 Ma. The different stages of plutonic activity and batholith growth along the Shyok Suture and eastern Karakoram may represent an example of stitching pluton and accretion of terrane between Indian and Asian plates.

Acknowledgements — *We are grateful to the Department of Science and Technology, Govt. of India, New Delhi for providing financial assistance under the sponsored Project No. ESS/CA/A9-32/93. We thank authorities at the Wadia Institute of Himalayan Geology, Dehradun for extending their support. Sincere thanks to Dr M.G. Petterson and three anonymous reviewers for their critical reviews and encouragement on an earlier version of manuscript which formed the base of present paper. Thanks are due to Drs P.P. Khanna, N.K. Saini of XRF and ICP-Labs of WIHG for analysing the volcanics and granitoid samples. Rb/Sr dates originated from PRL Ahmedabad, India under the guidance of Dr J.R. Trivedi. RU thanks the Federal Commission of Scholarships, Switzerland for providing a fellowship to carry out research at the Institute of Geology, ETH Zurich, Switzerland and to Professor Daniel Bernoulli and J.P. Burg for providing every kind of facility, support and encouragement at ETH Zurich.*

REFERENCES

Baldwin AJ & Pearce JA 1982. Discrimination of productive and non-productive porphyritic intrusions in the Chilean Andes. Economic Geology 77: 664-674.

Beck RA & 13 others 1995. Stratigraphic evidence for an early collision between northwest India and Asia. Nature 373 : 55-58.

Brookfield ME & Reynolds PH 1981. Late Cretaceous emplacement of Indus Suture Zone, ophiolitic melange and an Eocene-Oligocene magmatic arc on the northern edge of the Indian Plate. Earth Planet. Sci. Lett. 55 : 157-162.

Bonin B 1990. From orogenic to anorogenic settings: evolution of granitoid suites after a major orogenesis. Geol. J. 25 : 261-270.

Chappel BW & White AJR 1974. Two contrasting granite types. Pacific Geology 8 : 173-174.

Coward MP, Windley BF, Broughton RD, Luff IW, Petterson MG, Pudsey CJ, Rex DC & Khan AM 1986. Collision tectonics in the NW Himalayas. *In*: Collision Tectonics (Editors—Coward MP & Ries AC), Geol. Soc. Spec. Pub. 19 : 203-219.

Cox KG, Bell JD & Pankhurst RJ 1979. The interpretation of igneous rocks. George Allen and Unwin, London : 450.

Debon F & Khan NA 1996. Alkaline orogenic plutonism in the Karakoram Batholith: the Upper Cretaceous Koz Sar complex (Karambar valley, N. Pakistan). Geodinamica Acta 9 : 145-160.

Debon F & Le Fort PA 1983. Chemical-mineralogical classification of common plutonic rocks and associations. Trans. R. Soc. Edinburgh 73 : 135-149.

Debon F & Le Fort P 1988. A cationic classification of common plutonic rocks and their magmatic association: principles, methods, applications. Bull. Mineral. 111 : 493-510.

Debon F, Le Fort P, Dautel D, Sonet J & Zimmermann JL 1987. Granitoids of western Karakoram and northern Kohistan (Pakistan): a composite Mid-Cretaceous to Upper Cenozoic magmatism. Lithos 20 : 19-14.

Dietrich VJ, Frank W & Honegger K 1983. A Jurassic-Cretaceous island arc in the Ladakh Himalaya. Journal of Volcn. and Geothermal Res. 18 : 405-433.

Gaetani M 1997. The North Karakoram in the framework of the Cimmerian blocks. Him. Geol. 18 : 33-48.

Gansser A 1977. The great suture zone between Himalaya and Tibet, a preliminary account. Sci. Terre Himalaya, CNRS 268 : 181-192.

Henderson P 1984. Rare earth element geochemistry. Elsevier Science Pub. Amsterdam, Netherlands : 510.

Holtz F 1989. Importance of melt fraction and source rock composition in crustal genesis-the example of two granitic suites of northern Portugal. Lithos 24 : 21-35.

Honegger K, Dietrich V, Frank W, Gansser A, Thoni M & Trommsdorff W 1982. Magmatism and metamorphism in the Ladakh Himalaya (The Indus-Tsangpo Suture Zone). Earth Planet. Sci. Lett. 60 : 253-292.

Khan AM, Treloar PJ, Khan AM, Khan T, Qazi SM & Jan QM 1998. Geology of the Chalt-Babusar transect, Kohistan terrane, N. Pakistan: implications for the constitution and thickening of island-arc crust. Journal of Asian Earth Sciences 16 : 253-268.

Le Fort P, Michard A, Sonet J & Zimmermann JL 1983. Petrography, geochemistry and geochronology of some samples from the Karakoram Axial Batholith (northern Pakistan). *In* : Shams FA (Editor)–Granites of the Himalayas, Karakoram and Hindu Kush, Punjab Univ. Lahore, Pakistan : 377-387.

O' Connor JT 1965. A classification for quartz-rich igneous rocks based on feldspar ratios. US Geol. Surv. Prof. Paper 525B : B79-B84.

Ogasawara M, Watanabe Y, Khan F, Khan T, Khan MSZ & Khan KSA 1994. Late Cretaceous igneous activity and tectonism of the Karakoram block in the Khunjerab valley, northern Pakistan. *In* : Riaz A & Arshad MS (Editors)–Geology in South Asia-I. Proceed. First South Asia Geol. Congr., Islamabad 1992 : 203-207.

Pearce JA, Harris NBW & Tindle AG 1984. Trace element discrimination diagrams for the tectonic interpretation of granitic rocks. J. Petrol. 25 : 956-983.

Pearce JA & Norry MJ 1979. Petrogenetic implications of Ti, Zr, Y and Nb variations in volcanic rocks. Contr. Miner. Pet. 69 : 33-47.

Peccerillo A & Taylor SR 1976. Geochemistry of Eocene calcalkaline volcanic rocks from Kastamonu area, Northern Turkey. Contrib. Mineral. Petrol. 58 : 63-81.

Petterson MG & Windley BF 1985. Rb-Sr dating of the Kohistan arc-batholith in the Trans-Himalaya of north Pakistan, and tectonic implications. Earth and Planet. Sci. Lett. 74 : 45-57

Petterson MG & Windley BF 1991. Changing source regions of magmas and crustal growth in the Trans-Himalayas: evidence from the Chalt volcanics and Kohistan batholith, Kohistan, northern Pakistan. Earth Planet. Sci. Lett. 102 · 326-341.

Pudsey CJ 1986. The northern suture. Pakistan: margin of a Cretaceous island arc. Geological Magazine 123 : 405-423.

Rai H 1982. Geological evidence against the Shyok Palaeo-suture, Ladakh Himalaya. Nature 297 : 142-144.

Rai H 1991. The Shyok valley (Northern Ladakh, India): An entraped and compressed marginal oceanic basin. J. Him. Geol. 2 : 1-15.

Rakesh Chandra 1998. Tectonic framework and geologic feature of accreting back-arc of Hundri and Sasoma area between Shyok and Nubra river water divide, Ladakh Himalaya and Karakoram (J & K), India. Unpublished Ph.D. Thesis, Garhwal University Srinagar, India : 227.

Reynolds PH, Brookfield ME, Halifax G & McNutt RH 1983. The age and nature of Mesozoic-Tertiary magmatism across the Indus Suture Zone in Kashmir and Ladakh (NW India and Pakistan). Geol. Rundschau 72 : 981-1004.

Schorer U, Hamet J & Alleare CJ 1980. The Trans Himalayan (Gangdese) plutonism in the Ladakh region: a U-Pb and Rb-Sr study. Earth and Planet. Sci. Lett. 67 : 327-339.

Sharma KK 1990. Petrology, geochemistry and geochronology of the Ladakh Batholith and its role in the evolution of Ladakh magmatic arc. *In* : Sharma KK (Editor)–Geology and Geodynamic Evolution of the Himalayan Collision Zone, Physics and Chemistry of the Earth 17 (2) : 173-194.

Sinha AK, Trivedi JR, Upadhyay R, Rai H & Chandra R 1997. Geochemical and geochronological studies of granitoids of eastern Karakoram and their impact on the tectonic interpretation. Extended abstract in International Conference on Isotope in the Solar System (11-14 Nov., 1997), PRL Ahmedabad : 116-117.

Sinha AK & Upadhyay R 1997. Tectonics and sedimentation in the passive margin, trench, forearc and backarc areas of the Indus Suture Zone in Ladakh and Karakoram : a review. Geodinamica Acta 10 : 1-12.

Sinha AK, Rai H, Upadhyay R & Chandra R 1999. Contribution to the geology of the eastern Karakoram, India. Geol. Soc. America Spec. Pap 328 : 33-46.

Srimal N 1986. India-Asia collision: implications from the geology of the eastern Karakoram. Geology 14 : 523-527.

Srimal N, Basu AR & Kyser TK 1987. Tectonic inferences from oxygen isotopes in volcano-plutonic complexes of the India-Asia collision zone, NW India. Tectonics 6 : 261-273.

Sun S-S & McDonough WF 1989. Chemical and isotopic systematics of oceanic basalt: implications for mental composition and processes. *In* : (Editors– Saunders AD & Norry MJ) Magmatism in the Ocean Basins, Geol. Soc. Spec. Pub. 42 : 313-345.

Tahirkheli RAK, Mattauer M, Proust F & Tapponier P 1979. The India-Eurasia suture zone in northern Pakistan, some new data for an interpretation of plate scale. *In* : (Editors—Farah A & De Jong KA)–Geodynamics of Pakistan, Geol. Surv. of Pakistan, Quetta : 125-130.

Thakur VC & Mishra DK 1984. Tectonic framework of the Indus and Shyok suture zones in eastern Ladakh, northwest Himalaya. Tectonophysics 101 : 207-220.

Treloar PJ, Petterson MG, Jan QM & Sullivan MA 1996. A re-evalution of the stratigraphy and evolution of the Kohistan arc sequence, Pakistan Himalaya: implications for magmatic and tectonic arc-building processes. Journal of the Geological Society London 153 : 681-693.

Upadhyay R & Sinha AK 1998. Tectonic evolution of Himalayan Tethys and subsequent Indian Plate subduction along Indus Suture Zone. *In* : Proc. Indian National Science Academy (INSA), New Delhi 64 A : 659-683.

Upadhyay R, Sinha AK, Chandra R & Rai H 1999. Tectonic and magmatic evolution of the eastern Karakoram, India. Geodinamica Acta 12 (in press).

White AJR & Chappell BW 1977. Ultra-metamorphism and granitoid genesis. Tectonophysics 43 : 7-22.

Winchester JA & Floyd PA 1977. Geochemical discrimination of different magma series and their differentiation products using immobile elements. Chem. Geol. 20 : 325-343.

Zeitler PK 1985. Cooling history of the NW Himalaya. Tectonics 4 : 147-151.

Zen E- an 1986. Aluminium enrichment in silicate by fractional crystallization: some mineralogic and petrographic constraints. J. Petrol. 27 : 1095-1117.